TWO-PHASE FLOW WATER HAMMER TRANSIENTS AND INDUCED LOADS ON MATERIALS AND STRUCTURES OF NUCLEAR POWER PLANTS

(WAHALoads)

CO-ORDINATOR

Prof. Michel GIOT
UCL/TERM
Bâtiment Simon Stevin
2, Place du Levant
B – 1348 Louvain-la-Neuve
Belgique
Tel : +32(0)10.47.22.00
Fax : +32(0)10.45.26.92

LIST OF PARTNERS

1	UCL/TERM - Université catholique de Louvain	B
2	FZR - Forschungszentrum Rossendorf e.V.	D
3	UMSICHT - Fraunhofer Institut für Umwelt-, Sicherheits- und Energietechnik	D
4	AEKI/KFKI - Atomic Energy Research Institute	HU
5	FANP – Framatome Siemens	D
6	CEA/Grenoble, Département de Thermohydraulique et de Physique	F
7	IJS - Jozef Stefan Institute	SI
8	IBER - IBERDROLA s.a.	E
9	TBL - Tractebel s.a.	B
10	EA - Empresarios Agrupados Internacional	E
11	EdF - Electricité de France	F

CONTRACT N°: FIKS-CT-2000-00106

EC Contribution:	EUR 1,270,000
Total Project Value	EUR 2,176,317
Starting date:	October 2000
Duration:	42 months

Table of contents

Executive Summary

The project aimed at the elaboration of improved and innovative tools and methods for maintaining and improving the safety of existing reactor installations. The global objective was to predict the loads on equipment and support structures, which are caused by water hammers and shock waves. In particular, the following goals were set:

- review, evaluation and selection of existing experimental data;
- supply of new experimental data on water hammer using innovative two-phase flow instrumentation and including the measurement of loads on supports;
- supply of new experimental data on dynamic stresses in equipment walls;
- quantification of scaling effects by evaluating tests in different scales;
- development of new as well as improvement of existing condensation models to increase accuracy of thermal hydraulic modelling for water hammer calculations;
- development of a new 1D two-phase flow code for water hammer and shock wave transients in piping networks;
- validation of thermal hydraulic models including the new computer code for condensation-induced water hammers and shock waves in two-phase flows;
- qualification of 1D and 3D computational tools for the analysis of the structural response including fluid-structure interaction and validation of complex response models.

The project consisted of four work packages.

WP 1 dealt with experiments. Reference data were obtained at three different test facilities. Tests to characterise water hammers, shock waves and the resulting loads in relevant piping configurations with condensation effects were performed at two of these test facilities: Pilot Plant Pipework (PPP, scenario 2) and PMK-2. Together with additional data from the 1/1 scale UPTF facility, the process of condensation controlled water hammer has been studied at three different scales up to the plant scale. Additionally in the PPP facility (scenario 1), tests involving rapid valve closures have been performed. In the third test facility (Cold Water Hammer Test Facility), pressure waves typical for water hammers have been generated, and the resulting 3D stress fields on the pipe have been measured. The resulting original data bank consists of the following numbers of fully documented data:

- PPP scenario 1 : rapid valve closure: 94 runs
- PPP scenario 2 : cold water injection into steam: 3 runs
- PMK2 : cold water injection into steam: 35 runs
- CWHTF: 3D structural response to water hammer: 20 runs.

WP 2 dealt with thermal hydraulic modelling. A new code (WAHA code) has been built to examine the influence of the numerical methods on the water hammer predictions. It is based on a 6-equation, 1D, two-fluid model for transient non-homogeneous, non-equilibrium two-phase flow. Two main flow regimes (stratified and dispersed flows) are considered as well as the transition between them. The thermal non-equilibrium is modelled by a relaxation equation for the quality. A transient wall friction relaxation model based on Extended Irreversible Thermodynamics is available. A special treatment of the piping deformation has been introduced in the set of balance equations. It is based on an original development of the balance equations (mass, momentum and total energy) for a moving pipe of arbitrary cross-section. Forces can easily be obtained from the calculation results by using a simplified version, dedicated to fixed pipes, of the generalized formulation which was shown to be in

agreement with the usual standards. Advanced numerical methods for hyperbolic conservation laws are included in order to damp down the numerical diffusion effects. A separate integration scheme enables to accurately integrate the stiff source terms. Hydraulic forces can be easily obtained from WAHA thermal-hydraulics calculation on the piping system. A special study has been devoted to the modelling of the mechanical non-equilibrium between the phases by means of a physically based relaxation law.

During its development, the code has been tested against tests benchmark and other test cases.

In ***WP 3*****,** eight organisations took part in benchmark exercises, involving two types of codes:

- general purpose system codes, including a six equation two-fluid flow model with 1st order space and time integration, staggered mesh, and a library of fluid interface models based on flow regime maps;
- specialised fast transient codes, including the two-phase homogeneous equilibrium model; they are of the 2nd order in space and time.

It appeared that general purpose system codes that are not specifically designed for fast transients – are effectively not capable of capturing secondary waves due to vapour cavity collapse.

The benchmark exercises were found helpful for the first validation of the WAHA code and the new detailed data obtained on three the test facilities were used by the industrial partners for further verification of WAHA and of their own tools: CATHARE, DELOS, EUROPLEXUS, FLOWMASTER, MONA, RELAP5, ROLAST, and UMSICHT code. Fluid structure interaction effects have been studied using AGPIPE, ANSYS and EUROPLEXUS.

It is worth mentioning that the comparisons between the predictions and the data collected from the new complex experiments have substantially increased the level of expertise of the scientists involved in this project and the qualification of the codes used mainly by the industrial partners.

Finally, ***WP 4*** was devoted to the coordination of the project. It covered project management, preparation of the consortium agreement, quality assurance (preparation of a QA manual, and of a QA audit), and documentation. The use of a specific web site has revealed to be a very efficient communication tool and information sharing tool within the project.

This final report describes the work performed by the eleven partners of this challenging project during the whole duration of the contract. WAHALoads started on 1st October 2000. Upon request of the Co-ordinator, the project was prolonged by six months until March 2004.

The first section of the report gives the list of plenary meetings held during the project, and reports on the system of communications through Internet which has been specifically set up for the project. The status of the consortium agreement and of the publications is indicated in the next two sections. The main part of the report consists in sections 5 to 8 where the status of each work package is presented, including the main results. Section 9 summarises the status of deliverables, while section 10 presents the conclusions.

The deliverables consisting in a set of separate reports are considered as appendices of the present report. They can be found in the co-ordinator's directory of the WAHALoads web site, and can be downloaded by any partner and by the Commission. At the end of the project, a copy on DVD of all the directories of the WAHALoads web site was distributed to each partner. A copy of the Co-ordinator directory is transmitted to the European Commission.

The **implementation plan** involves the following three steps:

- In 2005, a workshop will be organised by the Consortium to inform the potential users in Europe and in the World about the results of the project: mainly the WAHA code and the new experimental data. In addition, in the framework of the Eleventh International Topical Meeting on Nuclear Reactor Thermal Hydraulics (NURETH 11, October 2-6, 2005, Avignon, France) two benchmark tests based on newly, unpublished experimental results obtained during the course of WAHALoads are proposed.
- It is agreed between the partners that the WAHA web site will remain active during at least a few years to facilitate further exchanges between the partners. By this means, it is foreseen to open new studies, new reports… to the original WAHALoads partners, and to promote master and doctoral theses.
- It is proposed that the WAHA code would be integrated in the NURESIM software platform (6^{th} FP). Several partners of WAHALoads expressed their wish to participate in NURESIM.
- We also plan to publish the main results of the program in Multiphase Science and Technology.
- Maintenance and developments of the WAHA code will be made on request of the industrial partners on a separate contract basis

A. Objectives and scope

1.1. Introduction

In existing NPPs water hammers can occur in case of an inflow of sub-cooled water into pipes or other parts of the equipment, which are filled with steam or steam-water mixture. They also may appear as the consequence of valve closing or opening actions or of breaks in pipelines, with single phase or two-phase flow. In the latter case, shock waves in two-phase flow must be expected. In all cases, strong dynamic stresses are induced in the wall of the equipment. Further, the change of the momentum of the liquid motion and the deformation of the component due to the dynamic stresses generate high loads on the support structures of the component, in which the water hammer respectively the shock wave occurs.

There are several scenarios were water hammers can take place. During normal operation, it may be caused by standard actions such as start-up or shut-down of systems and components, switch-over from one component (e.g. pump, heat exchanger) to another. There are also reports about water hammers during the execution of equipment test procedures requiring the activation of safety or auxiliary systems (e.g. by opening of valves). During transients, water hammer may occur as a consequence of the activation of emergency core cooling systems (ECC) or auxiliary feed water systems. Finally, breaks of high energy pipes possibly followed by rapid isolation valve closure may cause severe water hammers.

It must be guaranteed that the mechanical loads during water hammer and similar transients do not cause any damage of equipment and support structures. Water hammers are very infrequent events. It is not expected that they contribute to material ageing. They are nevertheless important with respect to ageing, because it is necessary to analyse the consequences of water hammers, when they act on equipment which is pre-damaged by other types of ageing, like thermal loads or corrosion. For the purpose of deciding when a component has to be replaced, an accurate prediction of the loads is necessary.

1.2. Objectives

The proposed project aims at the elaboration of improved and innovative tools and methods for maintaining and improving the safety of existing installations, in particular concerning light water reactors (LWR). The global objective is to achieve an accurate prediction of the loads on equipment and support structures of the installations of NPP, which are caused by shock waves occurring as a consequence of breaks and rapid valve movements, or by condensation-induced water hammers occurring as a consequence of an inflow of sub-cooled water into parts of the equipment, which are filled with steam. In particular, the following goals are set:

- review and evaluation of existing experimental data on steam condensation in contact with sub-cooled water (UPTF) and other fast transient two-phase flow data
- supply of new data on water hammer by carrying out experiments with an innovative two-phase flow instrumentation (transient void fractions, interfacial area, inter-phase heat transfer) including the measurement of stresses in walls and loads on supports
- supply of new experimental data on dynamic stresses in walls of the equipment with a complex geometry
- quantification of the influence of scaling on the thermal hydraulics of condensation of steam in contact with sub-cooled water by evaluating tests in different scales
- development of new as well as improvement of existing condensation models to upgrade existing thermal hydraulic codes in order to qualify them for water hammer calculations

- development of a one-dimensional computer code to simulate water hammer type fast pressure transients in piping and open networks, and to calculate the resulting hydraulic forces on the pipes, implementing new methods to suppress numerical diffusion and to improve the description of condensation
- validation of thermal hydraulic models including the new computer code for condensation-induced water hammers and shock waves in two-phase flows
- qualification of 1D and 3D computational tools for the analysis of the structural response including fluid-structure interaction and validation of complex response models to predict loads in structures and supports

The results enable a better understanding and an improved modelling of condensation-induced water hammer with respect to the thermal hydraulic effects of contact condensation, which control the load source, namely the dynamic pressure and the resulting fluid forces (new code + codes RELAP, MONA, PLEXUS, ROLAST-KWUROHR). It provides validated computer codes considering the fluid structure interaction and predicting the loads on the wall of the equipment and the supports (codes: PLEXUS, CIRCUS, ROLAST-KWUROHR, ADINA). It provides validated models and tools for considering structural response due to transient fluid loadings and predicting the loads on the wall of the equipment and the supports (codes: PLEXUS, CIRCUS, ROLAST-KWUROHR, ADINA). In the project, new experiments are using three existing experimental test facilities. At the Cold Water Hammer Test Facility CWHTF (FZR) for three-dimensional effects of fluid-structure interaction, the Pilot Plant Pipework PPP (UMSICHT) and the integral test facility PMK-2 (AEKI KFKI) are used for water hammer experiments at different scales and system pressures. The scale-up towards real nuclear power plants is achieved by using UPTF data.

2. Plenary meetings and the WAHALoads web site

Eight plenary meetings were held during the course of the project. They are:
- Kick-off meeting at Louvain-la-Neuve (UCL, Belgium) on October 10 – 11, 2000;
- First half year meeting at Oberhausen (UMSICHT, Germany) on March 12 – 13, 2001;
- Second half year meeting at Rossendorf (FZR, Germany) on October 4 – 5, 2001.
- Third half year meeting at Grenoble (CEA, France) on March 12 – 13, 2002;
- Fourth half year meeting at Ljubljana (IJS, Slovenia) on October 10 – 11, 2002;
- Fifth half year meeting at Budapest (AEKI, Hungary) on March 31st to April 2nd, 2003;
- Sixth half year meeting at Offenbach (FANP, Germany) on August 27 – 29, 2003.
- Seventh half year meeting at Madrid (EA, Spain) on March 1 - 3, 2004.

The minutes of these meetings are uploaded on the Co-ordinator directory of the WAHALoads web site: deliverables D1 to D6 for the first six meetings, D6b and D6c for the last two.

In addition to the plenary meetings, several meetings between partners specifically involved in complementary tasks have taken place during the project. These meetings were mainly related to instrumentation design for the experiments, and to selection of models and numerical methods for the WAHA code.

In order to facilitate the communications between the partners, a specific WEB site called WAHALoads has been used. Its address is : http://www.meca.ucl.ac.be/waha. The Web site involves a directory for each partner including the co-ordinator directory, and a directory for

the European Commission. All the official documents (deliverables, minutes of the plenary meetings, etc.) are uploaded in the Co-ordinator directory and accessible not only for every partner of the project, but also for the European Commission. The rules for uploading and downloading accesses, as well as other details related to the WAHALoads web site were indicated in the user's guide available on the WAHALoads web site itself and are reported in attachment 1 of deliverable D1.

3. Work performed and results

3.1. Work Package 1: Experiments on Water Hammers

3.1.1. Summary of WP1

The UMSICHT test facility **PPP** has been extended and improved with the installation of a new measurement technology including new wire mesh sensors with thermocouples for the measurement of condensation heat transfer and other innovative transient measurement techniques. This instrumentation was installed in PPP additionally to the existing one. The cold water test facility (**CWHTF**) of FZR was built and extended in order to perform fluid structural interaction effects at condensational hammers. The **PMK-2** test facility of KFKI/AEKI was extended by a steam-line model to study spontaneous water hammers appearing during feeding cold water into pipes filled with steam.

All experimental results give very precise data regarding both thermal hydraulic aspects and structural behaviour, which furthermore build an excellent basis for future work in code validation. This knowledge is the basis for more complicated experiment scenarios typical for power plant operation as well as for advanced software code and model validation.

3.1.2. Experiments at Fraunhofer UMSICHT test rig PPP

At Fraunhofer UMSICHT, the mechanism and the prediction of water and cavitational hammers were investigated by performing the following scenarios which are typical of conditions in power plants (**Fig.1**):

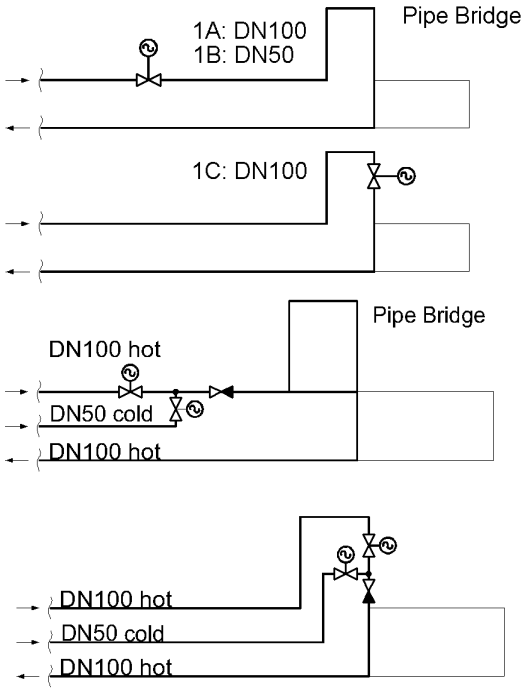

Scenario 1: *Water and cavitational hammer at increasing temperature (20°C - 180 °C)*

Scenario 2: A-B-C: Condensation hammer caused by cold water injection into steam

Fig.1. - Typical possible scenarios for the occurrence of pressure surges in power plants.

The typical scenarios for the origin of pressure surges are fast closing valves triggered by the breakdown of auxiliary power and fast acting control devices. For experiments according to scenario 1 the experimental set-up including the main measuring positions is given in **Fig.2**. The total test pipe length (from FP1 – FP3) was reduced from 215 m to 137 m in order to simulate typical power plant piping.

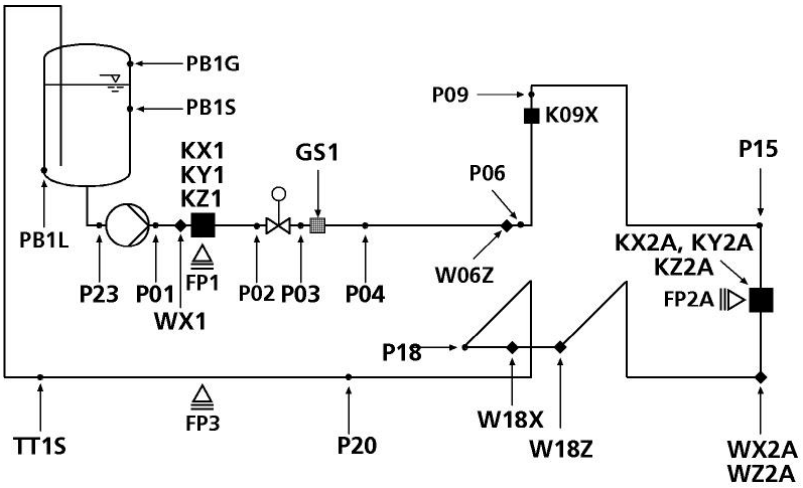

Fig.2. - Experimental set up for experiments according to scenario 1.

Hot water is pumped into the circuit from the pressurised vessel B1 into the test pipe section of 110 mm inner diameter. When the closure valve is closed rapidly (while the pump keeps running), pressure waves are induced in the whole pipe system and measured by fast pressure transducers (P01 – P23). Forces on pipe supports are measured (FP1 – 3) as well as displacements (W1 – 18). The measuring frequency is 2 kHz. Phase and temperature distributions are measured with a newly developed wire mesh sensor and local void probes (GS).

FSI effects are expected in the newly constructed pipe bridge 2 sections (**Fig.3**), where pipe support is quite elastic on the basis of typical pipe support conditions in power plants (**Fig.4**).

The experimental parameters are given in **Table 1**:

Table 1: Experimental matrix

Initial steady state velocity	$1.0 \leq v \leq 5$ m/s	5 velocities
Liquid temperature	$20 \leq \vartheta \leq 150$ °C	9 temperatures
Re-opening of valve after approx. 10 s	Yes / no	-
System pressure	1.0; 10 bar	2 pressures
Repetition of Experiments	At least 2 / experiment	-

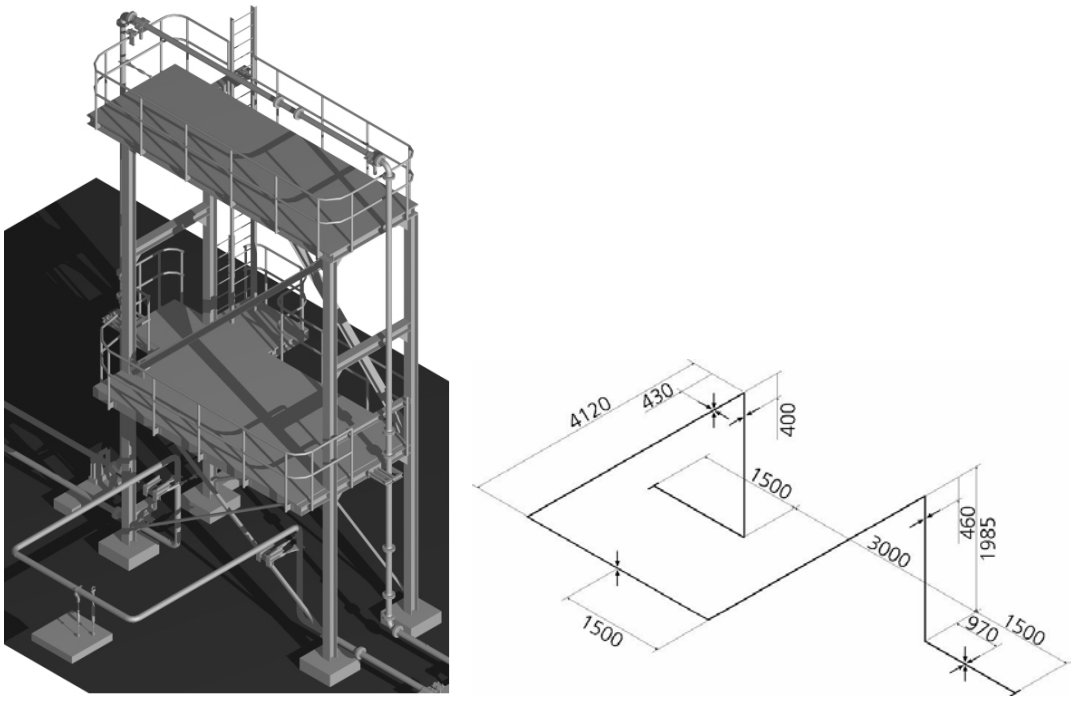

Fig.3 & 4. - : New construction of pipe bridge 2, extensions for FSI experiments and pipe support concept of new pipe bridge 2.

3.1.3. Advanced wire mesh sensor technology

Wire-mesh sensors are used to perform a high-speed visualisation of a gas-liquid two-phase flow. They consist of two grids of thin parallel wires which span over the measuring cross-section. The wires of both planes cross at an angle of 90° [deg.]. During the signal acquisition, one plane of electrode wires is used as transmitter, the other as receiver plane. The transmitter electrodes are activated by supplying them with voltage pulses in a successive order. The current at the receiver wire resulting from the activation of a given transmitter wire is a measure of the conductivity of the fluid in the corresponding control volume close to the crossing point of the two wires. The currents from all receiver wires are sampled simultaneously. This procedure is repeated for all transmitter electrodes. After activating the last transmitter wire, a complete matrix of measured values is filed in the computer. This matrix reflects the complete two-dimensional conductivity distribution in the sensor cross section at the time of measurement. The conductivity values are transformed into local instantaneous volumetric gas fractions by relating them to the conductivity of plain liquid and subtracting the result from the total. The resulting data is the basis for the fast flow visualisation and for the calculation of void profiles, bubble size distribution as well as for the performance of a decomposition of radial gas fraction profiles according to bubble size classes.

When applied in water hammer tests, mesh-sensors are used in which the wires were replaced by more stable electrode rods. The electrode rods are designed with a lenticular cross section, which helps reduce pressure drop and flow disturbance.

The sensors were redesigned for an operation at temperatures of up to 180 °C. In order to avoid damage of the electrode rods caused by thermal dilatation, the rods are fixed only at one side. The second side can slide in Teflon bushings when the temperature changes.

The second new feature is the introduction of micro-thermocouples. The ends of these micro-thermocouples are placed in special openings cut into the transmitter electrodes. The thermocouples are put into channels milled into the transmitter rods. The thermocouples themselves are laid through capillaries which are soldered into these channels, so that they can be replaced without destroying the sensor. The construction of a mesh sensor with 2 x 16 electrodes is shown in **Fig.5** and **Fig.6**. The lateral resolution given by the electrode pitch is 5.8 mm.

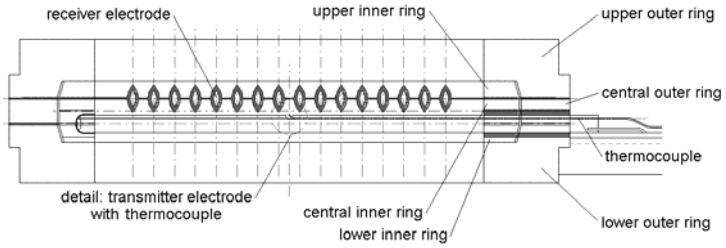

Fig.5. - Advanced mesh-sensor, 2x16 electrode rods, enlarged.

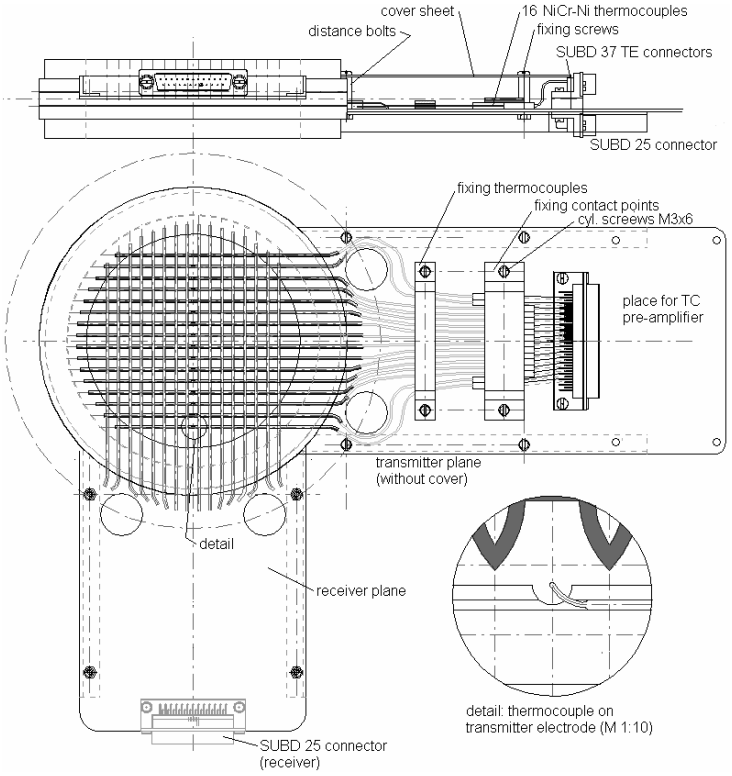

Fig.6. - Mesh-sensor DN100 with 2x16 electrode rods and 16 micro-thermocouples.

The temperature measurement is carried out at the same frequency as the void distribution measurement. A framing rate of 500 Hz was used in the presented measurements. The sensor was installed 231 mm downstream the fast acting valve. It was arranged in the way shown in **Fig.6**, i.e. the thermocouples were located along a vertical line in the centre of the measuring cross section. This arrangement was chosen to measure vertical temperature gradients which are likely to occur in the expected stratified flow.

3.1.4. Experimental results at PPP

This section gives an overview and an analysis of the results of the experiments related to thermal hydraulics and structure behaviour, conducted at UMSICHT using the PPP test facility. For a better comparison and in order to get more information about the cavitational hammer in various test parameters the results of void fraction measurements from the same experiments are also discussed.

Table 2: Experiments selected for the contribution

Experiment number	File name	Flowrate [m^3/h]	Liquid temperature [^oC]	Initial pressure B1 [bar]
135	132m020c01b00135d010	131.1	20.5	1.13
137	132m020c01b00137d010	132.8	21.2	1.12
262	132m080c01b00262d010	133.9	78.8	1.17
277	132m100c10b00277d010	134.8	99.5	10.02
307	132m120c10b00307d010	132.2	119.1	9.92
329	132m150c10b00329d010	131.0	146.6	10.18
396	132m080c10b00396d010	132.9	79.2	9.93

- ***Experimental results 1 – thermal hydraulics***

Fig.7 shows the pressure - time history for position P03 (also see **Fig.2**) at different temperatures. After valve closure at t = 0, the pressure decreases to saturation pressure because the liquid moves on. Thus big vapour bubbles are created. Since the pressure at the reservoir is constant, the liquid flows backwards; the bubble condenses downstream P03 at the (still closed) valve and causes a pressure peak (cavitational hammer) of approximately 45 bar.

A second cavitational bubble formed on the top of the pipe bridge keeps stable during the first 15 sec. Due to friction, de-aeration of air, and FSI, the process is repeated with decreasing effects. The initial temperature does not have a strong influence on the pressure up to t = 15 sec.

Error!

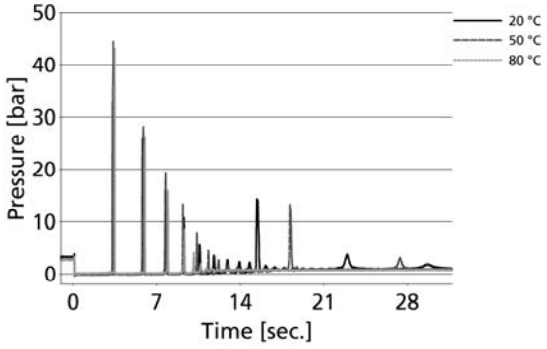

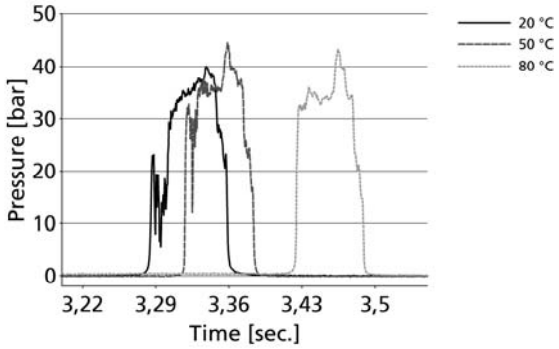

Fig.7b: First cavitational hammer at P03

Fig7a. Pressure peaks at p03

Fig.7. - Pressure peaks at P03 in dependency of temperature, v_0 = 4 m/s.

After 16 sec., further cavitational hammers are observed caused by the collapse of the vapour bubble on the bridge. **Fig.8** shows the time period (16 to 32 s) for the same experiments as shown in **Fig.7**. In **Fig.8**, the steady state temperature influences the height and the frequency of the cavitational pressure peaks.

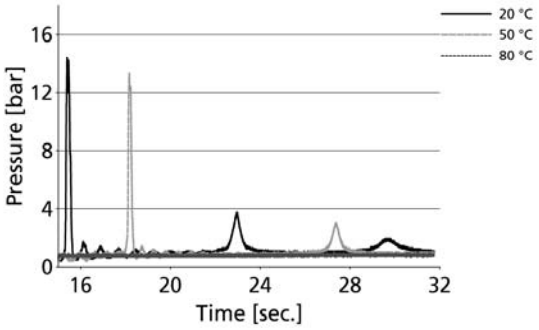

Fig.8. - Cavitational hammer in dependency of temperature due to collapse of the vapour bubble at P09 (pipe bridge).

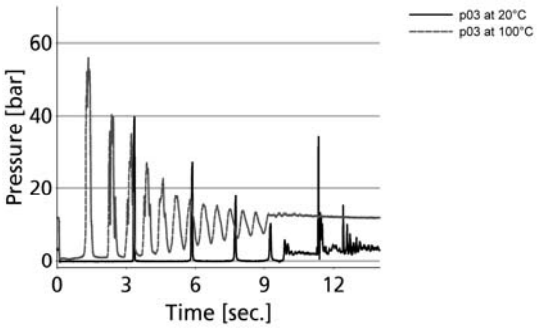

Fig.9. - Pressure time history of P03 at different temperatures and different initial pressures (run 137: 20 °C; 1bar; run 277: 100 °C; 10 bar).

As the temperature was increased further the system pressure was also raised in order to achieve an initial single phase flow in the whole pipe system. For a vessel pressure of 10 bar, the pressure time history at P03 is shown in **Fig.9** compared to conditions 1 bar / 20 °C. Due to the higher system pressure the first cavitational pressure peaks increase from 40 bar to approximately 58 bar. The higher peak also occurs much earlier because of the higher downstream vessel pressure. Furthermore, after re-opening of the valve at t = 11s, there is no collapse observed as at a pressure of 1 bar because the second bubble on the bridge has not formed yet.

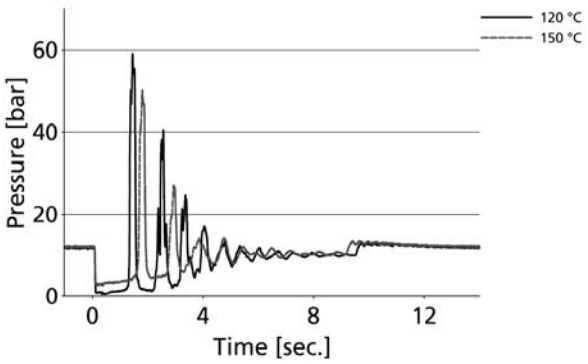

Fig.10.- Pressure time history at P03; initial velocity: 4 m/s, vessel pressure: 10 bar.

When the temperature is increased from 120 °C (test 00307) to 150 °C (test 00329) while the vessel pressure is kept constant (10 bar), saturation pressure increases while the cavitational hammer decreases due to the decreased speed of sound in liquid (**Fig.10**). The slowly increasing level of the saturation pressure during the first two seconds is an effect of the de-aeration of the liquid.

- ***Experimental results 2 – structural behaviour***

Fig.11 shows the time history of displacement and force measurements at different positions (see also **Fig.2**).

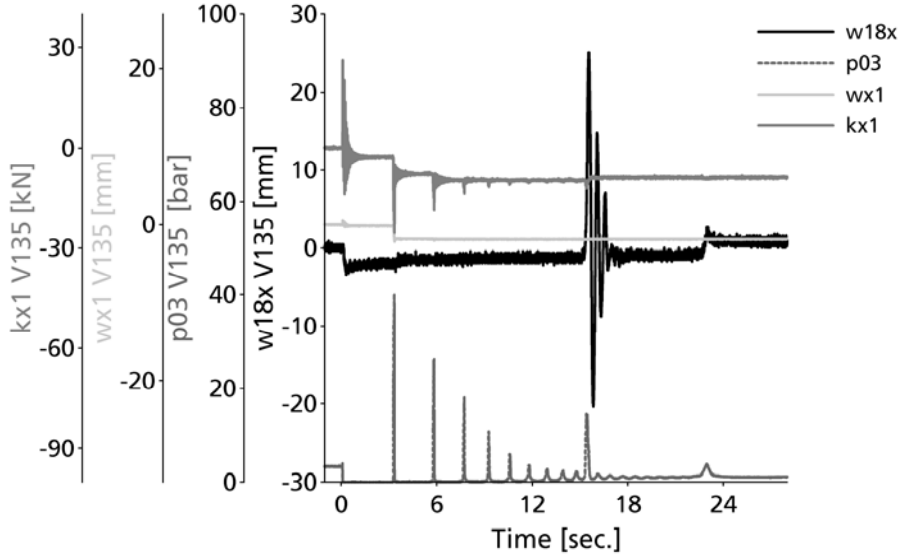

Fig.11. - Experiment V135 and the effect on structure: force and displacement measurements at different positions.

When the valve is closed, the initial low pressure wave downstream the valve leads to displacements in the whole system (w18x, wx1). With respect to w18x, the first cavitational hammer (t <15 s) does not affect the system downstream the pipe bridge, because the vapour bubble on the bridge divides the pipe hydraulically into two separate parts. Due to the

stiffness of the upstream part of the test rig (from vessel to pipe bridge), water hammer and cavitational hammer only lead to a low displacement although the forces induced at FP1 are quite high (approximately 40 kN). At the collapse of the vapour bubble on the bridge at t = 16 s, the second smaller pipe bridge (see **Fig.2.**) is moved up to 20 mm in axial direction.

- ***Results of void fraction measurements***

To enable visualisation, the two-dimensional distributions are transformed into a series of cross-section plots by converting local instantaneous gas fractions into colours according to a colour scale. The first steam appears at about 0.11 s when the valve is completely closed. The evaporation starts almost uniformly in the entire cross section, later on a stratified flow. This build up behaviour was observed in all valve closure experiments, as demonstrated in **Fig.12** for test 00307, which was performed at an initial temperature of about 120 °C.

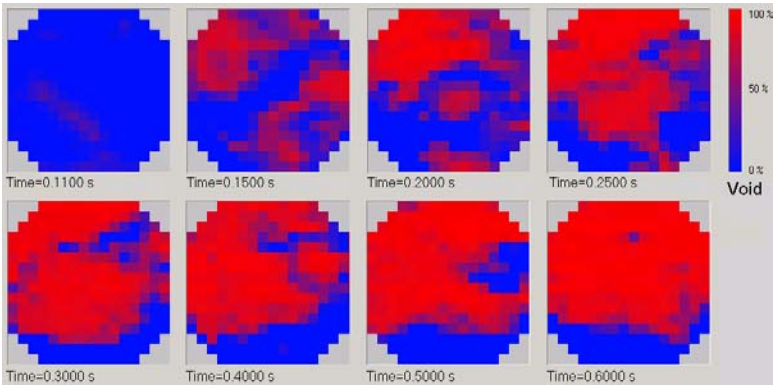

Fig.12. - Selected frames from a series of two-dimensional void fraction distributions in the first 0.60 s of the cavitation process in test run 00307 - Initial evaporation and onset of stratification.

Another instructive type of visualisation is obtained by plotting the time history of the local instantaneous void fractions measured at a vertical line in the centre of the sensor transformed into colours (**Fig.13**). The resulting coloured bars are stacked on top of each other. This results in an Eulerian sectional side view of the flow pattern. The histories of the axial void fraction distributions are plotted together with the pressure history downstream of the valve (p_{03}) as well as with temperatures measured in the cross section of the sensor by selected micro-thermocouples that were installed there. For a better understanding, the axial positions of the thermocouples, the signals of which were chosen, are indicated in the void fraction distributions. After the second pressure peak the pressure downstream of the valve does not reach the saturation pressure anymore. Bubbles observed later, are bubbles of previously dissolved air evolved due to the pressure decrease.

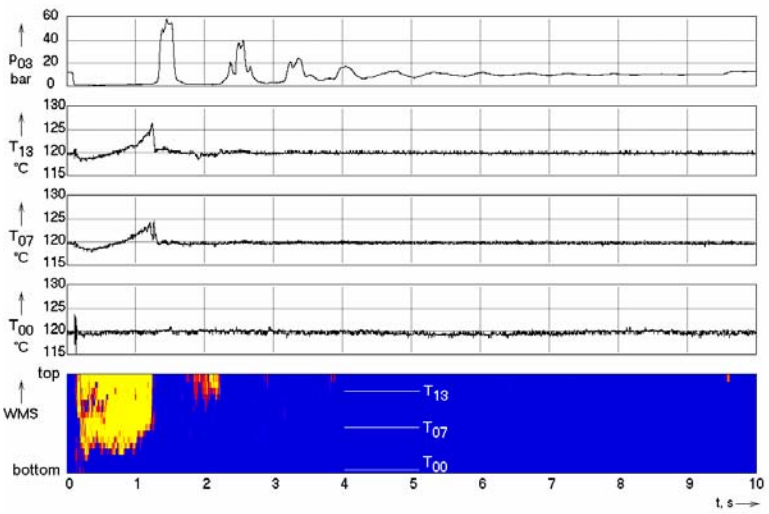

Fig.13. - Time histories of axial void fraction distribution, pressure downstream of the fast acting valve and selected temperatures from the micro-thermocouples inside the mesh sensor for test run 00307.

The process of expansion and compression for the test runs 00307 a performed at 119.7 °C respectively is shown in more detail in **Fig.14** , where a higher time resolution and a smaller pressure scale were used. Both temperature decrease during the expansion and the increase during compression are clearly visible. The behaviour of the temperature corresponds to the pressure tendency. The rise of the temperature is abruptly terminated when water arrives at the axial position of the given thermocouple.

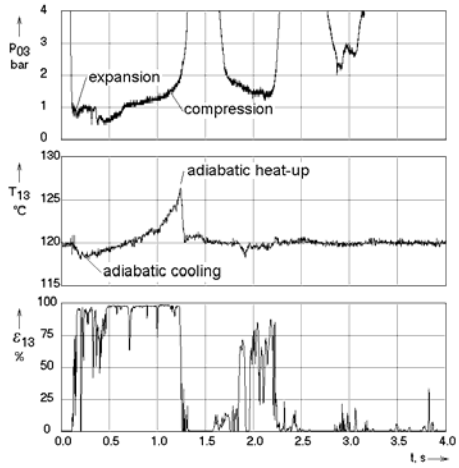

Fig.14.- Time-history of pressure downstream the fast acting valve during cavitation, temperature and local void fraction close to the top of the pipe section, test run 00307.

3.1.5. Experiments at PMK-2

- ***Description of the test facility***

The water hammer test section consists of a 2.87 m long horizontal pipe with an inner diameter of 73 mm designed for a maximum pressure of 16 MPa. It is supplied with steam from the dome of the steam generator model of PMK-2. The end of the test section is connected with the condenser unit of this test facility, which substitutes the turbine of the real plant. The design of the test section is shown in **Fig.15**.

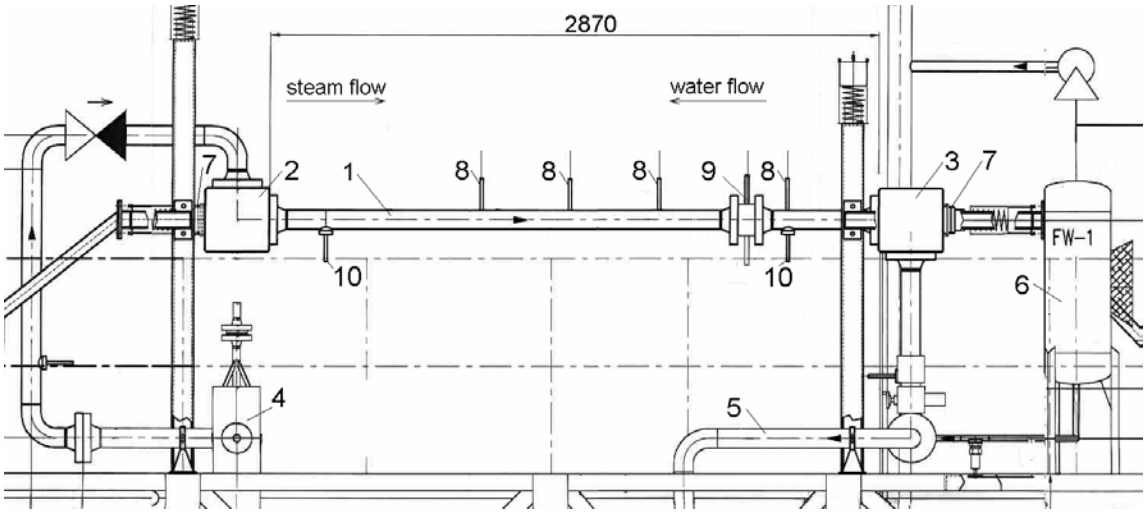

Fig. 15.- Experimental steam line for water hammer investigations at the PMK-2 test facility 1 - horizontal test section ∅73, 2 - inlet head, 3 - outlet head, 4 - steam generator head, 5 - connecting pipe to condenser, 6 - water tank, 7 - displacement cell, 8 - local void probe with integrated thermocouple, 9 - mesh sensor, 10 - pressure transducer.

Both ends of the test section are equipped with inertia blocks with a mass of 200 kg each, serving as 90 deg. bends in the same time. The test section can be isolated by two valves; one is located in the connection with the steam generator head, the other in the connecting line towards the condenser. For the supply of cold water, a water tank with a volume of 75 l is installed, which is pressurised with Nitrogen. The water injection is initiated by opening a valve in the injection line (inner diameter 24 mm).

The locations of mesh-sensor, needle probes and fast pressure transducers are indicated in **Fig.16**. For measuring the system pressure, the steam temperature and the steam respectively water flow rates the standard instrumentation of PMK-2 is used.

The sensor consists of two grids of 12 parallel electrode rods placed into the flow at a short distance behind each other. The void fraction distribution is obtained by relating the instantaneous conductivity distribution to the conductivity of the liquid phase. The time resolution is 1000 Hz.

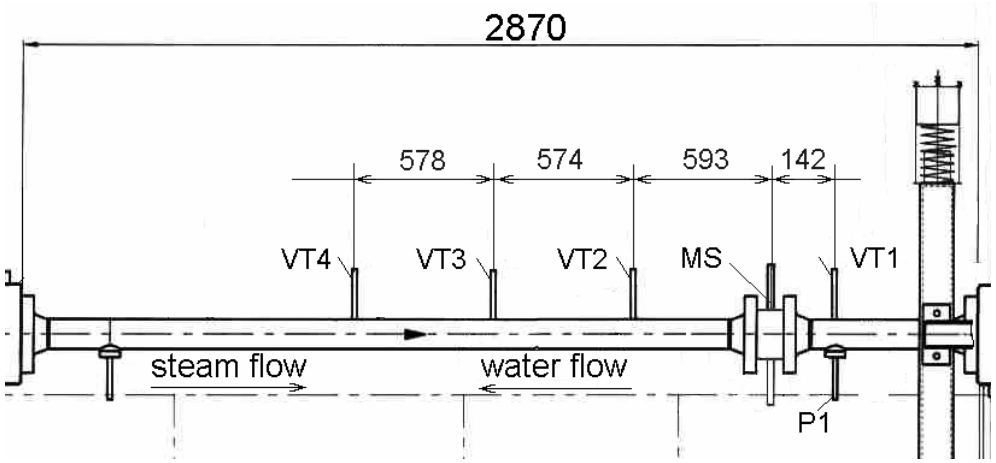

Fig.16.- Positions of the advanced void probes VT, the mesh sensor MS and the fast pressure transducer P1.

For the fast pressure measurements, three temperature resistant semiconductor transducers, type HEM-375M (KULITE SEMICONDUCTOR), with a measuring range of 50 MPa were applied. The transducers have a resonance frequency between 1120 and 1350 Hz. The test section was furthermore equipped with two electro-resistive strain gauges. They were mounted onto the outer surface of the test pipe and recorded the strain in two directions. The strain in the direction parallel to the pipe axis is called axial strain (S axial), the strain in the circumferential direction is called radial strain (S radial). Both fast pressure transducers and strain gauges are connected to a stand-alone data acquisition system ensuring a sampling frequency of about 5 kHz.

- ***Experimental results of tests AEKI_Exp03 - AEKI_Exp07***

Four experiments are described, the parameters of which are given in **Table 3**. In all cases, the test section was isolated from the steam generator after the heat-up and before the start of the cold water injection.

Table 3: Parameters of the reported tests at PMK-2

Run	Steam pressure	Water temperature	Water flow rate
	MPa	°C	kg/s
AEKI_Exp03	0.98	30	1.20
AEKI_Exp04	1.15	30	0.66
AEKI_Exp05	1.45	25	1.01
AEKI_Exp06	1.50	30	1.66

An overview of the signals obtained with the advanced two-phase instrumentation is given in the following Figures. Additionally, the readings of the fast pressure transducers and the strain gauges are plotted.

In all four test runs strong pressure peaks were observed. The highest pressure (18.35 MPa) was reached in test AEKI_Exp06 (**Table 4**). The table also contains the pressure

increase compared to the initial system pressure. The pressure peaks are very narrow; the typical pulse width is in the range of 1-2 ms (**Fig.17**).

Table 4: Observed pressure peaks

Run	Maximum pressure	Pressure increase
	MPa	MPa
AEKI_Exp03	12.99	12.01
AEKI_Exp04	2.75	1.60
AEKI_Exp05	17.43	15.98
AEKI_Exp06	18.35	16.85

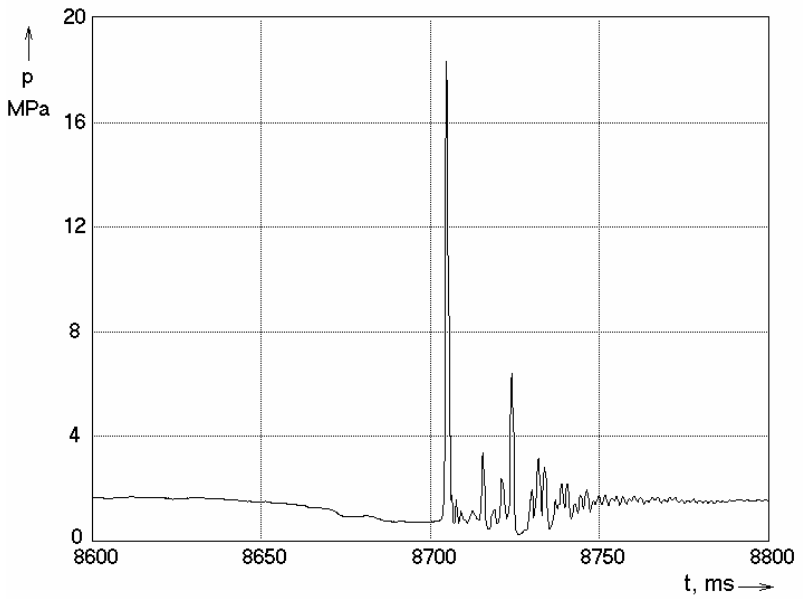

Fig.17.- Pressure history during the most intense water hammer observed (test run AEKI_Exp06), transducer close to the water inlet.

The flow phenomena during the experiments were visualised using the wire-mesh data (**Fig.18**). The calibration, i.e. the provision of reference values characterising the conductivity of the liquid phase is difficult, because the conductivity is temperature-dependent and the temperature itself varies due to the injection of cold water into saturated steam. For the calculation of void fraction distributions, the conductivity distribution in the first frame after the water hammer was taken as reference, since the pipe is then completely filled with water and the temperature distribution in the liquid phase is close to the one shortly before the water hammer.

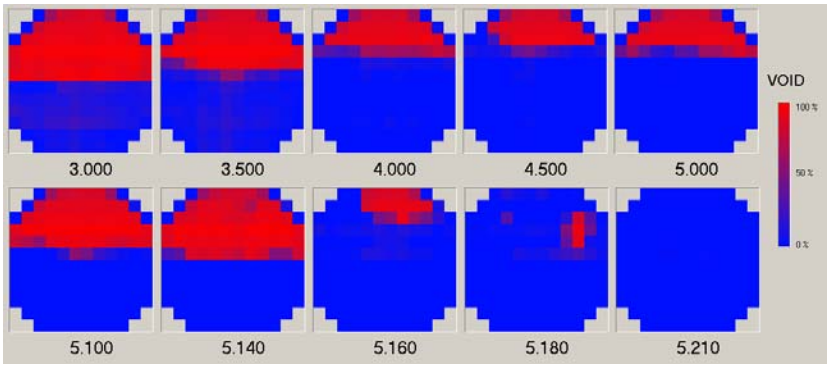

Fig.18.- Void fraction distributions measured by the mesh sensor, late fill-up phase and void collapse, experiment AEKI_Exp03.

In **Fig.18**, the void fraction distributions measured by the sensor are given for the last 2 seconds before the water hammer in experiment AEKI_Exp03. In the period from 3 to 4.5 s the water level is still increasing due to the feeding. Afterwards, in a comparatively short period of about 0.65 s, the level decreases again. This is a sign of the ongoing slug formation. In this period, the condensation process causes an increase of the vapour velocity, which leads to a displacement of water inside the test section. The sensor is located in a cross section from where water is dragged away. In the interval between 5.14 and 5.21 s the condensation collapse occurs.

3.1.6. Fluid-Structure Interaction Investigations during water hammer with the cold water hammer test facility CWHTF at FZR

For the experimental investigations of the fluid-structure interactions during water hammers at FZR, a cold water hammer test facility (CWHTF) was designed and built up (**Fig.19**). The CWHTF consists of a pressure vessel (tank), a pipeline with two straight sections (one horizontally and one vertically oriented), two 90° bends (curvature radius 306 mm) and a fast opening valve. The total length of the pipeline is about 3 meters; the outer pipe diameter is about 219 mm and the wall thickness 6 mm. The vertical pipe region is terminated by a lid flange which acts as a bouncing plate.

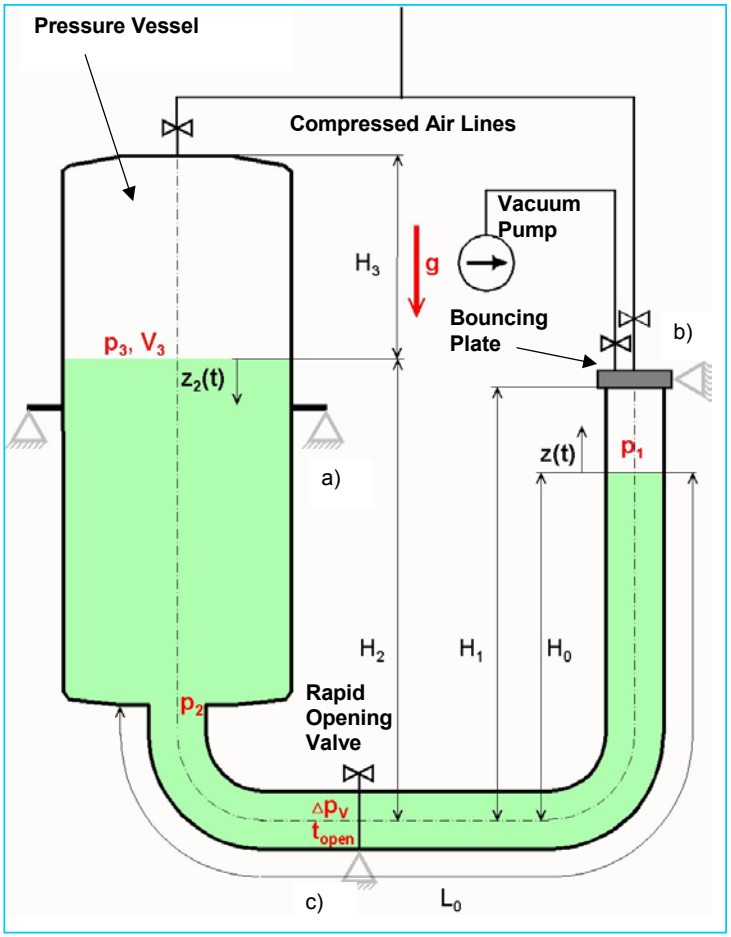

Fig.19.- Definition of the parameters of the CWHTF. Test parameter variations were made for: H_0, H_3, p_1, p_3, and t_{open}. Furthermore the fixation of the bouncing plate was varied; a) fixation vessel; b) fixation bouncing plate; c) fixation valve.

The water hammer is generated by the accelerated water bouncing against the lid flange. The water level in the vertical part of the pipeline is adjusted at a certain distance from the lid flange. The free volume above this level is evacuated ($p_1 << 1$ bar) through a hole in the bouncing plate. During this time the fast acting valve is closed. After a rapid opening of the valve the fluid is accelerated until bouncing against of the upper lid of vertical pipeline. At that time a water hammer is induced. The pressure p_3 in the tank may be increased by pressurized air (up to 5 bar) to increase the amplitude of the pressure waves generated. The

generated pressure wave travels back through the bend, causing a strong structural response of the pipe system.

The valve is connected to a spring mechanism which allows the quick opening of the turning plate within a defined time. The turning plate is supported in the horizontal middle plane of the pipe. The opening time can be varied between 0.02 and 0.5 s by changing the pre-stress of the springs. The opening mechanism is hydraulically initiated by loosing the arrest of the pre-stressed springs. This makes no counterthrust onto the pipe system, so the excitation of vibrations is rather low. Table 5 contains the main parameters of the CWHTF.

Table 5: Main parameters of the CWHTF		
Parameter	**Pipeline**	**Vessel**
Outer diameter	219 mm	800 mm
Wall thickness	6.0 mm	6.0 mm
Curvature radius of the bend	306 mm	-
Total pipe lenth L_0	3285 mm	-
Internal volume	125 dm³	750 dm³
Design pressure	60 bar	10 bar
Pressure of plastification	90 bar	-
Pressure of break	226 bar	-

The test results can be summarized as follows:

- in the straight pipe section the tangential strain signals correspond well with the pressure signals of the corresponding position;
- the increase of the evacuation pressure leads to a decrease of the pressure slope and of the pressure amplitude;
- the global bending of the CWHTF pipe system can be seen in the axial strain signals at the curvature; increasing evacuation pressure leads to decreasing strains;
- if the valve opening time is increased to more than 0.5 s a significant reduction of the pressure amplitude occurs and
- no influence of the acceleration on the pressure signal was measured.

The fluid-structure interaction occurring during a water hammer is characterized by two basic effects:

- The propagation of two coupled acoustic waves (the pressure wave in the fluid and the stress wave in the pipe wall); and
- The common vibrations of fluid and pipeline which are governed by global dynamic properties of the pipe depending on geometry, boundary conditions, material, wall thickness etc. this can be summarized under the term junction coupling.

3.1.7. References of WP1:

Prasser, H.-M., Böttger, A., Zschau, J., *"A New Electrode-Mesh Tomograph for Gas-Liquid Flows",* Flow Measurement and Instrumentation, 9 (1998) 111-119.

Dudlik, A.; Prasser, H.-M.; Schlüter, S., *"Visualization of cavitating liquid flow behind fast acting valve"*, ECCE 2 - Second European Congress of Chemical Engineering - Montpellier 05.-07.10.1999, paper CDROM 11270003.pdf.

Prasser, H.-M., Dudlik, A.; Schönfeld, S. B. H.; Fahlenkamp, H.; Schlüter, S., *"Prevention of Water Hammer in Pipelines in Case of Emergency Shut-Off by Fast Acting Valves",* ECCE-3, 3rd European Congress on Chemical Engineering, Nürnberg, 26.-28. Juni 2001, Proc. on CD-ROM, Poster P2 - 60.

Dudlik, A.; Hagemann, O.; Fahlenkamp, H.; Prasser, H.-M. *„Innovative Maßnahmen zur Vermeidung von Druckstößen und Kavitationsschlägen"*, 3R international, 39 (2000) 11, S. 673-677.

Dudlik, A.; Schönfeld, S. B. H.; Schlüter, S.; Fahlenkamp, H.; Prasser, H.-M., *"Prevention of Water Hammer and Cavitational Hammer in Pipeline Systems, Chemical Engineering and Technology"*, 2 (2002) Sept., pp. 888-890.

Neuhaus, T.; Dudlik, A.; Fahlenkamp, H. *"Examination of Numerical Methods and Physical Modelling of Condensation Induced Water Hammer Including Gas Release"* The Practical Application of Surge Analysis for Design and Operation, 9th International Conference on Pressure Surges, Chester 3/2004, pp. 569-580

Falk, K.; Bergant, A.; Dudlik, A.; Neuhaus, T.; Murray, S.J.; Pothof, I.; Hunt, S. *"Multi-phase Effects on Pressure Surge"* The Practical Application of Surge Analysis for Design and Operation, 9th International Conference on Pressure Surges, Chester 3/2004, pp. 661-672

Borga, A.; Ramos, H.; Covas, D.; Dudlik, A.; Neuhaus, T. *"Dynamic Effects of Transient Flows with Cavitation in Pipe Systems"* The Practical Application of Surge Analysis for Design and Operation, 9th International Conference on Pressure Surges, Chester 3/2004, pp. 605-617

Schönfeld, S.B.H.; Dudlik, A.; Neuhaus, T.; Schlüter, S.; Prasser, H.M. *"Pressure Surges in Pipe Systems: Impact on Plant Safety, Detection, Analysis and Prevention Methods"* to be published in Proceedings of CHISA 2004, Prag 8/2004

Dudlik, A.; Schönfeld, S.B.H.; Hagemann, O.; Fahlenkamp, H. *"Water hammer and cavitational hammer in process plant pipe systems"* KERNTECHNIK 68 (2003) 3, pp. 91-96

Dudlik, A.; Schönfeld, S.B.H.; Hagemann, O., Fahlenkamp, H. *"Water Hammer and Cavitational Hammer in Process Plant Pipe System"* Proceedings of 5th workshop on Measurement Techniques for Steady and Transient Multiphase Flows, Rossendorf (Dresden), Germany - September 18 - 20, 2002 ISSN 1437-322X

Dudlik, A.; Schlüter, S.; Hoyer, N. and Prasser, H.M. *"Pressure Surges - Experimental Investigations and Calculations with Software Codes"* 11th International Meeting of the IAHR Work Group on the behavior of hydraulic machinery under steady oscillatory conditions.

Bergant, A.; Dudlik, A.; Pothof, I.; Schoenfeld, S.B.H.; Tijsseling, A. *"CASE STUDIES OF FLUID TRANSIENTS IN SUBCOOLED PIPE FLOW"* Proceedings of the International Conference on CSHS03, Belgrade, 2003

Schönfeld, S.B.H.; Dudlik, A. *"Pressure Surges in Pipe Systems: Impact on Plant Safety, Detection, Analysis and Prevention Methods"* Beitrag zu International Trade Fair and Conference for Pipelines and Grids: Pipeline Automation +Control, 16th – 18th March 2004, München

Borga, A.; Ramos, H.; Covas, D.; Dudlik, A.; Neuhaus,T. *"DYNAMIC EFFECTS OF TRANSIENT FLOWS WITH CAVITATION IN PIPE SYSTEMS"* to be published in Proceedings of 9th International Pressure Surges Conference, Chester 2004

3.2. Work Package 2 : Modelling, Code Development

The goal of Work-Package 2 was the development of the computer code that can be used for simulations of the various mechanisms of single- and two-phase water hammer transients in piping systems. A computer code, called WAHA, was developed, which can simulate thermal-hydraulic transients with one-dimensional six-equation two-fluid model approximations and calculate forces on the piping. Five versions of the WAHA code were released within the WAHALoads project from October 2000 to March 2004 :

- **WAHA-Single-Phase** (October, 2001) was a preliminary version of the code, where the basic data structures and numerical methods were merged with input and output processing. WAHA-Single-Phase was capable to simulate single-phase transients with ideal gas as a working fluid in one-dimensional network of pipes with variable cross-sections (Tiselj et. al., 2001).
- **WAHA0** (October, 2002) was a first version of the WAHA code that was based on the six-equation two-fluid model. However, the code did not contain correlations for the description of inter-phase heat, mass, and momentum transfers. The special model of the abrupt area change developed for WAHA-single-phase was upgraded for the two-phase flow, while no model of branch was still available. New water property subroutines were developed and applied in WAHA0. The code manual contained only instructions for the input file preparation (Gale and Tiselj, 2002).
- **WAHA1** (June, 2003) contained the part of the numerical scheme for the integration of the stiff inter-phase heat, mass, and momentum transfers. Some first correlations for two basic flow regimes (dispersed and horizontally stratified) were available. The code manual contained the description of all equations, of the numerical scheme, of the abrupt-area change model, of the water property subroutines and of the input preparation instructions (Tiselj et. al., 2003).
- **WAHA2** (November, 2003) contained improved heat, mass, and momentum transfer correlations, which were tested against various test cases. A new chapter with the description of various test cases was added to the manual (Tiselj et. al., 2003).
- **WAHA3** (March, 2004) was the final version of the WAHA code released within the WAHALoads project. A model of the branch - connection of three pipes in a single point - is available in this version. A new model of the unsteady wall friction developed by B. Kucienska (2004) was adopted for the use in the WAHA code. WAHA3 can calculate forces on the pipes, assuming a rigid piping system (Tiselj et. al., 2004). WAHA3 consists of ~11000 FORTRAN lines, is described in a manual of ~190 pages (Tiselj et. al., 2004), and comes with a collection of 30 input files (including the test facilities used within the project). The main features of the latest WAHA3 code are given in section 6.1 below.

Section 6.2 describes another work that was being performed within the WAHALoads Work-Package 2: the formal background for the possible future upgrade of the WAHA code into the Fluid-Structure-Interaction code is described in detail in the report "Two-fluid 1D-averaged model equations for a pipe undergoing arbitrary motions" prepared by H. Lemonnier (2004). The fluid-structure-interaction, which means coupled simulation of the thermal-hydraulic process in the pipe and of the mechanical response of the pipe, was beyond the scope of the WAHALoads project. However, due to its importance for water hammer transients, it may appear in some of the future versions of the WAHA code.

3.2.1. Computer code WAHA

- ***Basic equations and physical models***

The six-equation two-fluid model was chosen as a basic mathematical model of WAHA. The simpler five-equation two-fluid model was eliminated because the assumption of vapour being in saturation conditions was found to be too limiting for condensation induced water hammers. The seven-equation two-fluid model with different phase pressures was rejected because of the unknown relations between both pressures. The basic equations are one-dimensional mass, momentum and energy balances for vapour and liquid, without terms for wall-to-fluid heat transfer:

$$\frac{\partial A(1-\alpha)\rho_f}{\partial t} + \frac{\partial A(1-\alpha)\rho_f(v_f - w)}{\partial x} = -A\Gamma_g, \quad \textbf{(1)}$$

$$\frac{\partial A\alpha\rho_g}{\partial t} + \frac{\partial A\alpha\rho_g(v_g - w)}{\partial x} = A\Gamma_g, \quad \textbf{(2)}$$

$$\frac{\partial A(1-\alpha)\rho_f v_f}{\partial t} + \frac{\partial A(1-\alpha)\rho_f v_f(v_f - w)}{\partial x} + A(1-\alpha)\frac{\partial p}{\partial x} - A\cdot CVM - Ap_i\frac{\partial\alpha}{\partial x} = AC_i|v_r|v_r - A\Gamma_g v_i + A(1-\alpha)\rho_f g\cos\theta - AF_{f,wall}, \quad \textbf{(3)}$$

$$\frac{\partial A\alpha\rho_g v_g}{\partial t} + \frac{\partial A\alpha\rho_g v_g(v_g - w)}{\partial x} + A\alpha\frac{\partial p}{\partial x} + A\cdot CVM + Ap_i\frac{\partial\alpha}{\partial x} = -AC_i|v_r|v_r + A\Gamma_g v_i + A\alpha\rho_g g\cos\theta - AF_{g,wall}, \quad \textbf{(4)}$$

$$\frac{\partial A(1-\alpha)\rho_f e_f}{\partial t} + \frac{\partial A(1-\alpha)\rho_f e_f(v_f - w)}{\partial x} + p\frac{\partial A(1-\alpha)}{\partial t} + \frac{\partial A(1-\alpha)p(v_f - w)}{\partial x} = AQ_{if} - A\Gamma_g(h_f^* + v_f^2/2) + A(1-\alpha)\rho_f v_f g\cos\theta, \quad \textbf{(5)}$$

$$\frac{\partial A\alpha\rho_g e_g}{\partial t} + \frac{\partial A\alpha\rho_g e_g(v_g - w)}{\partial x} + p\frac{\partial A\alpha}{\partial t} + \frac{\partial A\alpha p(v_g - w)}{\partial x} = AQ_{ig} + A\Gamma_g(h_g^* + v_g^2/2) + A\alpha\rho_g v_g g\cos\theta. \quad \textbf{(6)}$$

Standard notations are used in the above equations: p denotes the pressure, α the vapour volume fraction, v the velocity (m/s), e the specific total energy, ρ the density, C_i the inter-phase drag coefficient, θ the inclination of the pipe, v_i the velocity of the interface, Γ_g the vapour generation term, h^* the specific enthalpy, Q_{if}, Q_{ig} the heat fluxes from interface to phase f or g , and one uses subscripts f for liquid and g for vapour (where pi is defined and discussed at eq. 10). Differential terms are collected on the left-hand side of the equations and the non-differential terms are collected on the right. Pipe cross-section A can vary as a function of coordinate x and time:

$$A(x,t) = A(x) + A_e(p(x,t)), \qquad \frac{dA_e}{A(x)} = \frac{D}{d}\frac{dp}{E} = K\,dp \tag{7}$$

The A_e term takes into account the elasticity of the pipe walls (E is the pipe elasticity module, D the pipe diameter, and d the pipe wall thickness), which modifies the propagation velocities in the elastic pipes and is especially important when modelling water hammer transients.

Additional closure relations:
1) Two additional equations of state are needed to close Eqs. (1) - (6). The equation of state for phase k is:

$$d\,\rho_k = \left(\frac{\partial \rho_k}{\partial p}\right)_{u_k} d\,p + \left(\frac{\partial \rho_k}{\partial u_k}\right)_p du_k \tag{8}$$

Derivatives on the right hand side of Eq. (8) are determined by the water property subroutines developed for the WAHA code using pressure and temperature (T) or specific internal energy (u) as input. Properties - including metastable states - are interpolated from the pretabulated data at ~400 pressures (0 - 1000 bar) and 475 temperatures (273.15 - 1638 K). Some types of simulations are also possible for two-phase flows of liquid water and ideal gas without inter-phase heat and mass transfer.

2) The virtual mass term CVM in Eqs. (3) and (4) is used to achieve hyperbolicity of the equations in dispersed flow:

$$CVM = (1-S)C_{vm}\,\alpha\,(1-\alpha)\,\rho_m\left(\frac{\partial v_g}{\partial t} + v_f\frac{\partial v_g}{\partial x} - \frac{\partial v_f}{\partial t} - v_g\frac{\partial v_f}{\partial x}\right) \tag{9}$$

The value of coefficient C_{vm} was tuned to ensure the hyperbolicity of the two-fluid model equations (see Tiselj and Petelin, 1997 for details). The applied virtual mass term does not ensure unconditional hyperbolicity of the equations. For very large relative velocities (comparable to sonic velocity) complex eigenvalues may appear. However this did not happen for any of the physical test cases used during the WAHA code development.

3) The interfacial pressure term exists only in stratified flow:

$$p_i = S\alpha(1-\alpha)(\rho_f - \rho_g)gD \tag{10}$$

where S represents a stratification factor (S=0 for dispersed flow, S=1 for horizontally stratified flow, 0<S<1 for transitional flow - see Tiselj et. al., 2004 for details). This term enables to describe the surface waves in horizontally stratified flows.

4) The WAHA code distinguishes two flow regimes: the dispersed flow and the horizontally stratified flow, with a transition area between both regimes. The source terms are flow regime dependent and their detailed form is given in the WAHA manual (Tiselj et. al., 2004). The terms that do not include derivatives - source terms - are:

4.1) Terms with C_i - inter-phase drag.

4.2) Terms with Γ_g, Q_{ig}, Q_{if} - inter-phase exchange of mass and energy with:
$\Gamma_g = -(Q_{if}+Q_{ig})/(h_g-h_f)$ - vapour generation term,
$Q_{if} = H_{if}(T_s-T_f)$, $Q_{ig} = H_{ig}(T_s-T_g)$ - interface heat transfer terms,

H_{if}, H_{ig} - liquid-interface and gas-interface heat transfer coefficients.

4.3) Terms due to the variable pipe cross-section.

4.4) $F_{f,wall}$, $F_{g,wall}$ - wall friction.

4.5) Term with $g\,cos\theta$ - volumetric forces.

4.6) Terms for wall-to-fluid heat, mass, and momentum transfers are neglected in the WAHA3 code.

The coefficients which appear in the heat, mass, and momentum transfer correlations for horizontally stratified flows are derived from "standard" (Mills, 1999) correlations for a flow near a flat wall. The heat and mass transfer model for dispersed flow is derived from the Homogeneous Relaxation Model (Lemonnier, 2002), with the additional assumption of a very large gas-interface heat transfer coefficient for the vapour H_{ig}. The inter-phase drag for dispersed flows is modelled with correlations valid for bubbly and droplet flows. The criterion for the transition from horizontally stratified to dispersed flow is based on the onset of the Kelvin-Helmholtz instability.

5) The axial velocity of the structure w in Eqs. (1)-(6) is set to zero in the current version of the WAHA code and is foreseen for a possible upgrade of the WAHA code into the Fluid-Structure-Interaction code - see discussion in Section 6.2.

- ***Numerical scheme of the WAHA code***

The numerical scheme of the WAHA code is based on Godunov characteristic upwind methods. These schemes produce solutions with a substantially reduced numerical diffusion and allow the accurate modelling of flow discontinuities. Equations (1) to (6) can be written in a vectorial form as:

$$\mathbf{A}\,\frac{\partial \vec{\psi}}{\partial t} + \mathbf{B}\,\frac{\partial \vec{\psi}}{\partial x} = \vec{S} \qquad (14)$$

where $\vec{\psi} = (p, \alpha, v_f, v_g, u_f, u_g)$ represents the vector of the independent variables, matrices $\underline{\mathbf{A}}$ and $\underline{\mathbf{B}}$ represent matrices in front of derivatives of $\vec{\psi}$, and $\vec{S}$ the vector of sources. WAHA solves the basic equations in a non-conservative form. Numerous tests were performed with the six-equation model (described by Tiselj and Petelin, 1997) with different basic variables, and the most successful set of variables turned out to be $\vec{\psi} = (p, \alpha, v_f, v_g, u_f, u_g)$. The preferred set of variables would be conservative variables $\vec{\varphi} = [(1-\alpha)\rho_f, \alpha\rho_g, (1-\alpha)\rho_f v_f, \alpha\rho_g v_g, (1-\alpha)\rho_f e_f, \alpha\rho_g e_g]$ with specific total energies $e = u + v^2/2$. A conservative form of equations usually means also numerical conservation of mass, momentum and energy. However there are some specific problems with the conservative formulation of multi-fluid two-phase flows:

1) The continuity and energy equations can be written in the conservative form, while the fluxes for the momentum equations do not exist, due to the pressure gradient terms, the virtual mass terms, the interfacial pressure terms, and possibly other correlations that contain derivatives. The momentum equations thus cannot be written in the conservative (flux) form.

2) Oscillations appear in the vicinity of particular discontinuities, if complex systems of equations are solved with conservative variables (Tiselj and Petelin, 1997). These oscillations do not depend on the numerical scheme accuracy and can be observed in the results of the first and second-order schemes.

3) "Non-standard" water property subroutines are required that calculate the two-phase properties

$$(p, \alpha, \rho_f, \rho_g)$$

from the conservative variables

$$((1-\alpha)\rho_f, \alpha\rho_g, (1-\alpha)\rho_f u_f, \alpha\rho_g u_g).$$

According to our experience, non-conservative variables present an acceptable approximation for fast transients while for the long transients, where conservation of mass and energy is more important, this might be a serious drawback. In the test calculations presented in the WAHA code manual (Tiselj et. al., 2004), negligible fluctuations of the overall mass and energy have been observed despite the non-conservative scheme.

Due to the stiffness of the relaxation (inter-phase exchange) source terms, the WAHA code uses a two-step operator splitting to solve Eq. (14):

1) Convection and non-relaxation source terms - source terms due to the smooth area change, wall friction and volumetric forces are solved in the first sub step:

$$\mathbf{A}\frac{\partial \vec{\psi}}{\partial t} + \mathbf{B}\frac{\partial \vec{\psi}}{\partial x} = \vec{S}_{NON\_RELAXATION} \tag{15}$$

Equation (15) is solved with a characteristic upwind numerical scheme, which is based on the explicit evaluation of the eigenvalues of the Jacobian matrix $\mathbf{C} = \mathbf{A}^{-1}\mathbf{B}$ of the system:

$$\mathbf{C} = \mathbf{L} \cdot \mathbf{\Lambda} \cdot \mathbf{L}^{-1} \tag{16}$$

The diagonal matrix $\mathbf{\Lambda}$ is the matrix of eigenvalues and $\mathbf{L}$ is the matrix of eigenvectors of matrix $\mathbf{C}$. The eigenvalues, the eigenvectors, and the inverse matrix of the eigenvectors are numerically calculated between the grid points in the WAHA code. An upwind discretisation of the spatial derivatives is then performed in the space of the characteristic variables. A second-order accurate scheme is obtained with implementation of the slope limiters. The upwind discretisation and the slope limiters are used also for the calculation of the non-relaxation source terms in Eq. (15) (details in Tiselj et. al. 2004). Such approach preserves the steady-state solutions - for example, steady flow in ducts with a variable cross-section, or steady-state flows in vertical pipes with presence of gravitation.

2) The relaxation source terms are integrated in the second sub-step of the operator splitting method:

$$\mathbf{A}\frac{d\vec{\psi}}{dt} = \vec{S}_{RELAXATION} \tag{17}$$

The relaxation source terms - inter-phase heat, mass and momentum exchange terms - are stiff, i.e., their characteristic time scales can be much shorter that the time scales of the hyperbolic part of the equations. The integration of the relaxation sources within the operator-splitting scheme is performed with variable time steps, which depend on the stiffness of the source terms. Upwinding is not used to calculate the relaxation source terms. The properties of the operator splitting used in the WAHA code are described by Tiselj and Horvat (2002).

- ***Special models in WAHA code***

Unsteady wall friction: The comparisons of numerical with experimental results show that the simulations of the fast transients made with a steady friction formula often do not give good results. The passage of a water hammer wave has a significant influence on the velocity gradient at the wall, which is not taken into account in the steady-state friction models. Therefore the transient friction effect was included into WAHA code in the form of the Friction Relaxation Model developed by B. Kucienska, M. Giot, and J.M. Seynhaeve at the Université Catholique de Louvain (details in the doctoral thesis of B. Kucienska, 2004). The Friction Relaxation Model integrates two steps of the shear stress τ evolution that appears in the pipe after the passage of the pressure wave:

$$\frac{d\tau}{dt} = \frac{\tau_s - \tau}{\theta} + k_T \frac{\Delta w}{\Delta t} \qquad \textbf{(18)}$$

The second term on the right hand side takes into account the rapid change of the velocity gradient at the wall immediately after the passage of the pressure wave. The first term on the right hand side represents the relaxation of the shear stress associated with the evolution of the velocity profile to the steady-state profile corresponding to the new value of the average velocity behind the pressure wave.

An approximation of the Friction Relaxation Model was applied in WAHA. The approximated Friction Relaxation Model is a kind of a numerical solution of the exact model expressed by a differential equation. It is based on the shear stress value at the previous time step:

$$\tau(t) = \tau_s(t) + \tau_{un}(t)$$

$$\tau_{un}(t) = \tau_{un}(t - \Delta t) e^{\frac{-\Delta t}{\theta}} + k_T \Delta v \qquad \textbf{(19)}$$

where Δt is a time step and Δv is a difference between the velocity values at the two last time steps. The total shear stress at every time step is a sum of the steady shear stress τ_s and the unsteady contribution τ_{un} based on its value from the last time step. Initially: $\tau_{un}(0) = 0$.

Abrupt area change model: this model included in the WAHA code is recommended when the cross-section of the pipe is suddenly increased or decreased for a factor of two or more, since the smooth area change model built into the basic WAHA equations often fails in such situations. The model is based on the following assumptions:
- Steady-state balance conditions for the conservative variables across the area change (marked with $k \rightarrow n$ in **Fig.20**);
- No generation of mass, momentum and energy at the at the area change;
- Characteristic velocity based extrapolation of the quantities at the area change.

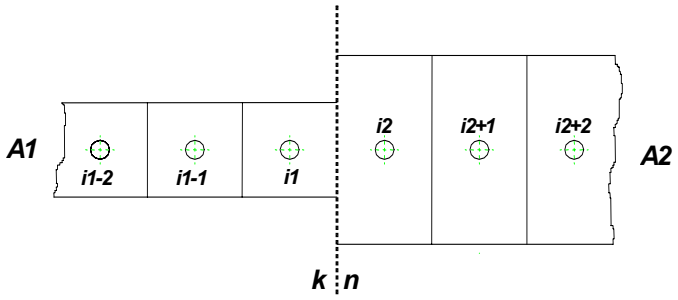

Fig.20. - Abrupt area change model.

The set of non-linear equations at the area change surface is solved with a Newton-Raphson iteration.

A branch model is applied when three pipes are connected in a single point. The branch does not have a volume; it is only a point that connects three pipes. The WAHA branch model is a slightly modified version of the approaches described in (Martin and Wiggert, 1996 and Wylie and Streeter, 1978). In the branch model the "dominant" pipe is first defined. The "dominant" pipe is defined as the pipe with the largest mass flow rate. The state in the other two connected pipes is averaged. For example, in the case where the main pipe is a pipe that has the index $i = 1$, the averaged pressure is calculated as:

$$p_{av} = \frac{p_2 A_2 + p_3 A_3}{A_2 + A_3}$$

The boundary values in the pipes are then calculated in the same way as in the abrupt area change model of pipes 1 and 2 with $\vec{\psi}_1 \leftarrow \vec{\psi}_{main}$, $\vec{\psi}_2 \leftarrow \vec{\psi}_{av}$ and $A_2 \leftarrow (A_2 + A_3)$.

When the abrupt area change calculation is finished, the boundary values in the dominant pipe 1 are already prescribed, while the values of the averaged pipe are taken as boundary values of pipes 2 and 3, except for the phase velocities, which are not taken as the velocity of the averaged pipe, but are extrapolated from pipes 2 and 3.

The available **Boundary conditions** at the end of the pipe in WAHA code are:

- Closed end;
- Constant pressure (tank) boundary condition; and
- Constant velocity (pump) boundary condition.

- ***Input/output processing of the WAHA code***

An example of a simple input model for the WAHA code is an ASCII file shown in Fig.21. The lines that start with " * " are comment lines and other lines present data cards. A card "time" specifies beginning and end time of the simulation and frequency of output of various output files and restart file. A card "time" specifies the gas phase: vapour or ideal gas, order of accuracy (first or second) of calculation, type of abrupt area change model and details of the data in the output file. The lines that start with "comp" describe components - pipes. Two pipes are defined in input in **Fig.21**: the first one is 3 meters long, has a cross-section of 0.4 m2, and is discretised in 75 volumes. The second one is 2 meters long, has a cross-section

```
title abrupt area change model test - contraction- two-phase mixture
* works for cross.sect-ratios 20:1 to 1:5
*--------time constants----------------------------------
*      beg     end     maj_out   min_out      diff        restart
time00 0       1.0e-2  2.0e-4    1.0e-4       0.80        2.
*      fluid   order   abr_model eig_val_out  extend_out  maj_results
switch 1       2       3         0            0           1
*-------------pipes   -------------------------------
*          type     name
comp001ty  pipe     cev_01
*          length   elast     thick     rough   w.fr.f  p.fr.f   h.m.tr.  nods
comp001g0  3.0      0.0       1.588e-3  0.0     9       0        0        75
*          cross    incl      azim      f_coeff node
comp001g1  0.4      0.0       0.0       1.0     75
*          type     press     alpha_g   velf    velg    uf       ug       wch_nods
comp001s0  agpvu    1.5e7     0.5       0.0     0.0     1.5853e6 2.4556e6 50
+          agpvu    1.0e7     0.9       0.0     0.0     1.3935e6 2.5452e6 75
*          from     to
comp001c0  000-00   005-01
*-----------------------------------------------------
*          type     name
comp005ty  pipe     cev_05
*          length   elast     thick     rough   w.fr.f  p.fr.f   h.m.tr.  nods
comp005g0  2.0      0.0       1.588e-3  0.0     9       0        0        50
*          cross    incl      azim      f_coeff node
comp005g1  0.02     0.0       0.0       1.0     50
*          type     press     alpha_g   velf    velg    uf       ug       wch_nods
comp005s0  agpvu    1.0e7     0.9       0.0     0.0     1.3935e6 2.5452e6 50
*          from     to
comp005c0  001-99   000-00
************************************************************
*
end
```

Fig.21. - Example of WAHA code input file.

of 0.02 m2, and is discretised in 50 volumes. The initial conditions are defined in cards "compXXXs0": pressure ($1.5*10^7$ Pa → 10^7 Pa) and vapour volume fraction jumps (0.5→0.9) are present in the first pipe at time zero. This input file was used to test the abrupt area change model of the WAHA code. The new users of the WAHA code are advised to use one of the 30 existing input files as a pad for preparation of a new input.

Several WAHA code output files are available: most of the data are found in the general output file, where the inconsistencies from the input processing are also reported. The useful output format are so called "major output" files with a snapshot of the state at given time. "Minor output" file is used for tracking of the temporal development of the chosen variables at the desired points in the system. The restart files of the WAHA code are written in the form of the input file, but with initial conditions that represent the state in the pipe at the time of the restart output. The calculation and output of the forces on the piping are performed in a separate file where 3D force vectors are printed at each hydrodynamic volume boundary.

- ***WAHA test cases and results***

Some results obtained with the WAHA code are available in WAHA code manual (Tiselj et. al., 2003) with a brief overview of the test cases used during the code development given below:

1) Single-phase gas and liquid tests:

- **Ideal gas shock tube** (Sod's problem) – The initial conditions in the pipe represent two uniform states separated by a discontinuity in various variables (Riemann problem). This test case gives an impression about the magnitude of the error in a strong shock wave propagation velocity due to the non-conservative numerical scheme.
- **Vapour shock tube** - Riemann problem for single-phase vapour.

- **Liquid shock tube** – The test case shows that errors due to the non-conservative numerical scheme are almost negligible for shock waves in a single-phase liquid.
- **Critical flow of ideal gas** - Another test of non-conservative numerical scheme in variable cross-section geometry. For given inlet and outlet pressures of a convergent-divergent nozzle and zero velocity initial conditions, WAHA predicts the development of the critical mass flow rate very similar to the analytical solution, but cannot predict steady the shock wave that appears at the position of the transition from supersonic to subsonic flow in the divergent part of the nozzle.
- Development of a **hydrostatic pressure field in a vertical pipe** - Liquid and vapour single-phase cases.
- **Abrupt area change models in single-phase flow**s - Abrupt contraction or expansion, liquid or vapour.
- **Branch behaviour in single-phase liquid and vapour flow** - Example in **Figs. 22 and 23**.

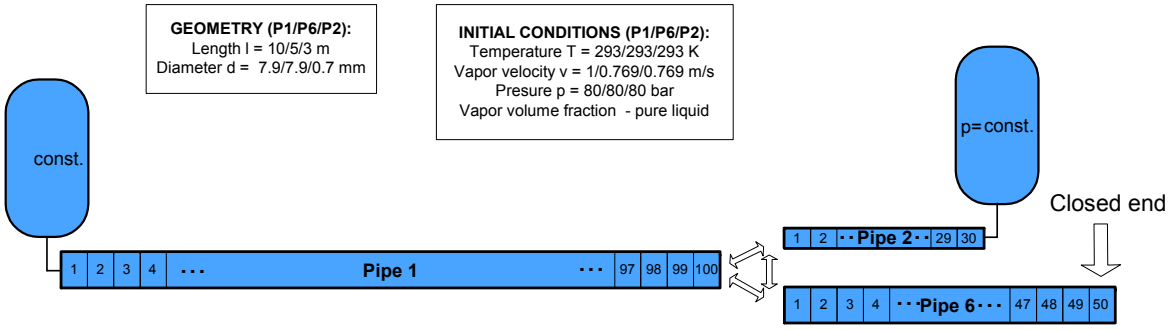

Fig.22. - Geometry and initial conditions of a test model of the branch filed with pure liquid.

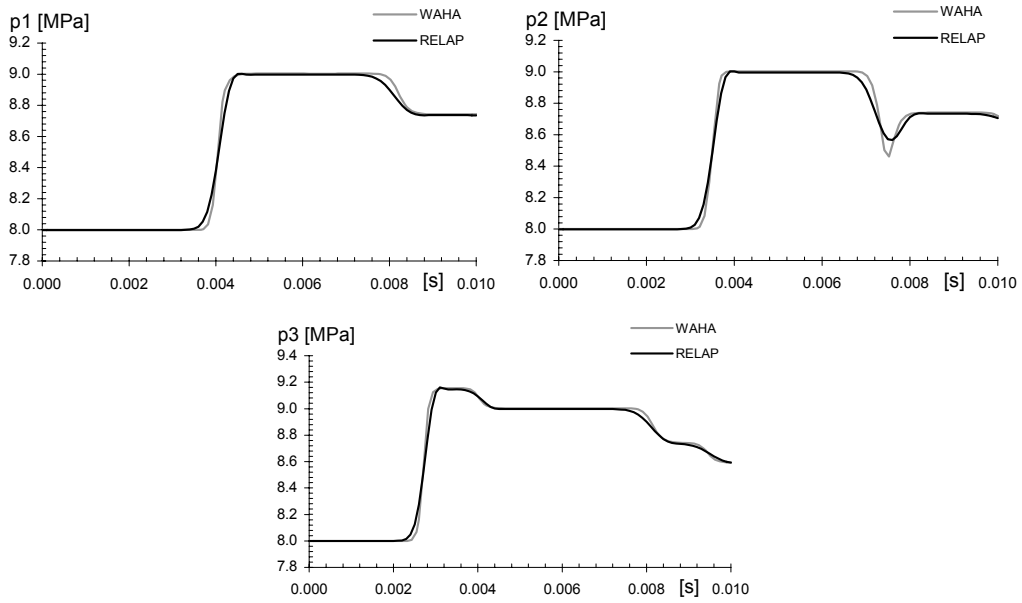

Fig.23. - Comparison of the WAHA and RELAP5 codes: pressure histories at points 1 (Volume 90 of pipe 1), 2 (Volume 2 of pipe 2) and 3 (volume 10 of pipe 6).

2) Two-phase test cases - Cases that do not represent models of actual experimental devices:
- **Two-phase shock tube** - non-realistic initial and boundary conditions - basic test of the numerical scheme in two-phase flow.
- **Abrupt area change models** in two-phase flow (expansion, contraction).
- **Separation of liquid and gas in vertical pipe** (two cases: with and without mass transfer). Test of the procedure for the integration of the non-relaxation source terms.
- **Oscillations of the liquid column** in a U-tube - test of the (non-)conservation properties with a "slow" transient (**Fig.24**). This test is important due to the periodic transitions from single-phase liquid into the single-phase vapour.

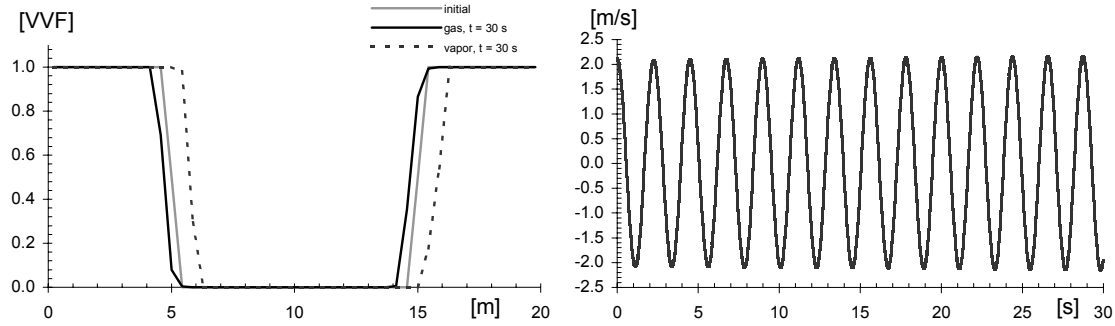

Fig.24: Vapour volume fractions at t=0 s, t = 30 s and liquid velocity history at the bottom of the U-tube.

- **Faucet problem** - Non-realistic initial and boundary condition: acceleration of the liquid column with air in vertical pipe.
- **Velocity of the small surface waves in horizontally stratified flow** - Basic test of the stratified flow equations.
- **Slug propagation** - Test of basic numerics and models for transition from single-phase liquid to single-phase vapour flow.
- **Dam-break problem** - Test of the stratified flow model with large surface waves.

3) **Two-phase flow experiments** – They are mainly discussed in the next chapter of the present report:
- **Edwards pipe** - Discharge of a hot liquid from a horizontal pipe - very important test - all correlations and models are tested. The expected agreement with the experiment was obtained.
- **Critical flashing flow in the Super Moby Dick nozzle**: The achieved steady-state solutions are in very good agreement with the experiments.
- **Simpson's valve closure water hammer** (one of the WAHA benchmark test cases).
- **UMSICHT valve closure initiated water hammer** (WAHALoads experiment, Dudlik and Prasser, 2003).
- **FZR Cold Water Hammer Test Facility** (WAHALoads experiment, Altstadt et. al., 2002).
- **Steam induced water hammer experiment performed at AEKI** (WAHALoads experiment, Szabados et. al. 2003). **Figs. 25 and 26** present the simplified geometry of the AEKI device modelled in the WAHA code, and the WAHA results for experiment no.5 from the final AEKI report D12.

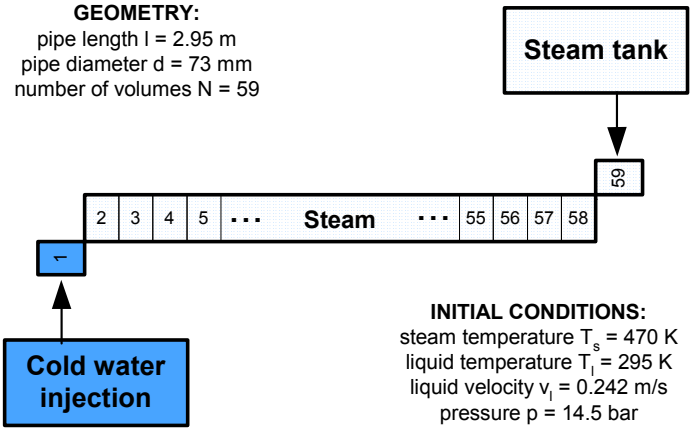

Fig.25. - Simplified geometry and initial conditions of experiment no. 5 on the AEKI device as modelled in the WAHA code. Measured pressure peak: 173 bar.

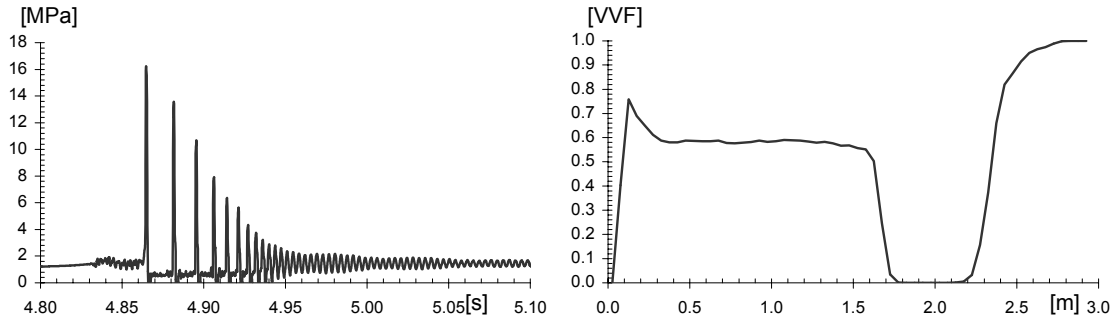

Fig.26. - WAHA predictions of the pressure history in volume 9 of the AEKI pipe, and vapour volume fraction profile just after the formation of the slug in the pipe.

As the AEKI experiment is very sensitive to the small initial conditions, the exact predictions of slugging onset and water hammer pressure peak are very difficult to obtain. Moreover, large uncertainties are observed in the experiment. The WAHA code exhibits very similar properties as the experiment; indeed, very small modifications of the inter-phase heat, mass and momentum transfer correlations produce very different results. The most important point for this type of water hammer event is that WAHA can predict the condensation induced water hammer, which occurs in the horizontally stratified flow after the formation of the slug and condensation of the entrapped bubble. Further correlation improvements are expected with respect to the AEKI experiment.

3.2.2. Formulation of the procedures for the possible upgrade of the WAHA code with Fluid-Structure-Interaction models.

Fluid and structure interactions were studied all along the project. Sample calculations in a simplified geometry have shown (Lemonnier, 2002) than “chaining” a fluid load calculation (typically from WAHA) with a structure calculation to get its motion was possible and that iterating the process was converging towards a solution. This solution shows a modulation of the water transients by the faster structure motion with the occurrence of rather realistic and well defined mechanical load peaks.

In order to make this coupling possible in future versions of WAHA, it has been necessary to re-formulate the two-fluid 6-equation model in a frame moving with the pipe considered as a beam with sections moving perpendicularly to the beam neutral fibre. The fallouts of these series of studies are summarized by Lemonnier (2004).

The calculation of the hydrodynamic loads taking into account the pipe motion, considers it is a given input. Future versions of WAHA will therefore have to consider include the pipe motion (displacement, mainly) into the input data set. Furthermore, it has been shown that the fluid equations were only slightly modified by the motion of the pipe, and that the resulting force on the piping can be deduced from similarly to the standard force calculation.

- ***Fluid equations***

The basic starting point is the averaging of the single-phase local equations over the fraction of the pipe section occupied by each phase. These equations involve various integrals that must be transformed to get the evolution equations of averaged quantities on the flow section such as the pressure, the velocity and the enthalpy. Two special forms of the Leibniz rule and of the Gauss theorem are necessary to operate this transformation and to produce the basis for the separate mass, momentum and total energy balances for each phase.

This so called two-fluid, six-equation model specialized for pipes moving with arbitrary motions is expressed in the natural geometrical frame of the moving and distorting pipe: the Fresnet frame involving the tangential direction along the pipe, $\boldsymbol{t}$, and two other directions lying in the pipe section namely, the normal, $\boldsymbol{n}$, directed towards the centre of curvature of the pipe and the binormal, $\boldsymbol{b}$, perpendicular to both the tangent and the normal vectors.

The main difficulty in justifying the use of a single scalar momentum equation for each phase comes from the non rectilinear nature of an arbitrary piping. In the case of a straight pipe, there is no argument on the way to produce this equation: the momentum balance is simply projected along the pipe direction together with the usual so called flat profile 1D assumption. In our work, these two steps have been extended. In the extended 1D approximation, it is mainly assumed that the only significant and independent flow velocity component is aligned with the instantaneous tangent, $\boldsymbol{t}$, and that the two other velocity components, in the Fresnet frame, are those of the pipe motion and are therefore given. The resulting momentum equation is projected along the three basis vectors ($\boldsymbol{t}$, $\boldsymbol{n}$, $\boldsymbol{b}$) and it results three scalar equations in only one unknown, the fluid velocity along the pipe direction. These equations are naturally expressed with the arc length along the pipe, s, as a space variable. This coordinate is not very practical since with a moving and therefore extending pipe, ends, probes are not located at fixed values of, s, at any time. An additional change of variable is necessary and the proposed choice is to use a Lagrangian coordinate for the pipe, s_0, the arc length along the initial (undistorted) pipe. The resulting equations are therefore expressed in a fixed spatial coordinate and involve only one scalar component of the flow velocity. The two extraneous equations will be used later since they encompass the force information.

Formally, the generalized mass, momentum and energy balances resemble very much the well known two-fluid model equations. The main differences are the following:

- The space variable is the arc length along the pipe.

- The space derivative terms are slightly modified by a geometrical scale factor essentially close to 1. This scale factor accounts for the local elongation of the pipe during its motion.
- The convective terms are slightly modified; they involve the velocity difference between the fluid and the structure motion instead of the fluid velocity only.
- The motion of the pipe is responsible for various acceleration terms that are calculated precisely by Lemonnier (2004). Their most important property is that they are analogous to volume force terms (gravity) and can be treated numerically in the same way. Though they are time varying they only depend on the known pipe motion.

Finally, the fluid equations are very similar to those of section 6.1 and the only minor modifications listed above are of geometrical nature which do not need to change the basic solving scheme of the equations. The practical calculation of the various geometrical quantities of interest has also been attempted by Lemonnier (2004).

- ***Forces***

Mechanical loading of the structures are deduced from the known wall forces acting on the fluid. The very simple reasoning of the standard force calculation cannot be reproduced here directly for the general case. Indeed, the standard force calculation relies on the use of an overall momentum balance applied to *fixed* and finite section of pipe. Since in the general case, the pipe is moving, some kind of added mass effect is expected and cannot obviously be obtained from the standard calculation considering a fixed pipe. It is another interest of the proposed formulation to obtain the forces with the same assumptions as those of the fluid motion with no extra calculations.

The basic principle consists in analysing the mixture momentum balances obtained by summing up each corresponding phasic equations. In these equations the action of the wall on the two-phase mixture appears explicitly and it can be isolated to provide the fluid reaction load on the pipe.

In the first version of the force model development, Lemonnier (2004) considered separately and differently the forces in the tangential and normal directions. The reasons were basically that for closing the momentum equation in the tangential direction an explicit model is needed and it was therefore thought unnecessary to reconstitute wall friction from the acceleration terms integrated other a pipe finite length. However, this procedure was utilized for the two other normal components of the force and as a result of our extended 1D assumption, they only involve known quantities.

The actual force calculation in WAHA relies on the standard force calculation. This is justified because up to now, the pipe is considered as fixed. By revisiting this method, it has been shown that volume forces were not included and they had been included in the WAHA code. In a second version of the force formulation, it is shown that the forces acting on the pipe can be cast in a form similar to that of the standard fixed pipe calculation. The main differences are the following:

- The forces are expressed in the Fresnet frame instead of the Cartesian frame. Projecting back to Cartesian frame is straightforward.

- The acceleration terms in the force expressions are similar to those for the fixed pipe and the extra acceleration terms have the same form than gravity and can be treated in the same way.

The details of the derivations and the practical application are detailed by Lemonnier (2004).

3.2.3. References of WP2:

Altstadt, E., Carl, H., Weiss, R., "*CWHTF data for code validation"*, WAHALoads project report, Deliverable D26, revision 0, Forschungszentrum Rossendorf, 2001.

Dudlik, A., *"Data Evaluation Report on PPP water hammer tests, cavitation caused by rapid valve closing"*, WAHALoads project report, Deliverable D35, Revision June, 2003, Fraunhofer Institut Umwelt-, Siecherheits-, Energietechnik UMSICHT, 2003.

Gale, J., Tiselj, I., Chapter on input preparation for WAHA0 code, WAHALoads project, October, 2002.

Kucienska, B., *"Friction Relaxation Model for Fast Transient Flow"* Université catholique de Louvain (UCL) Doctoral thesis, June 2004.

Lemmonier, H., *"An attempt to apply the homogeneous relaxation model to the WAHALoads benchmark tests with interaction with the mechanical structure"*, CEA-T3.3-D61-200302, WAHALoads project deliverable D61, 2002.

Lemonnier, H., *"Two-fluid 1D-averaged model equations for a pipe undergoing arbitrary motions"*, WAHALoads deliverable D31, CEA report 2002-043, Revision 2, 2004.

Martin, C.S., Wiggert, D., *"Waterhammer and Fluid Structure Interaction in Piping System"*, ASME Professional Development Programs, April 4.-5., p. 1-8, 1996.

Mills, A.F., *"Heat transfer"* 2nd edition, Prentice Hall, 1999.

Szabados, L., Baranyai, G., Guba, A., Ézsöl, Gy., Perneczky, L., Tóth, I., Trosztel, I., *"PMK-2 handbook, technical specification of the Hungarian integral test facility for VVER-440/213 safety analysis and steam line water hammer equipment"*, WAHALoads report, Deliverable D46, Draft, Atomic Energy Research Institute, 2001.

Tiselj, I., Petelin, S., *"Modelling of Two-Phase Flow with Second-Order Accurate Scheme"*. Journal of Computational Physics, 136, 503-521, 1997.

Tiselj, I., Černe, G., Parzer, I., Horvat, A., *"WAHA code development interim report - WAHA single phase code"*, WAHALoads project, Deliverable D63 version Oct. 2001.

Tiselj, I., Horvat, A., *"Accuracy of the operator splitting technique for two-phase flow with stiff source terms"*, Proceedings of ASME Joint U.S.-European Fluids Engineering Conference, Montreal, 2002.

Tiselj, I., Horvat, A., Černe, G., Gale, J., Parzer, I., Mavko, B., Giot, M., Seynhaeve, J.M., Kucienska, B., Lemonnier, H., *"WAHA1 code manual"*, deliverable D10 of the WAHALoads project, version June 2003.

Tiselj, I., Horvat, A., Černe, G., Gale, J., Parzer, I., Mavko, B., Giot, M., Seynhaeve, J.M., Kucienska, B., Lemonnier, H., *"WAHA2 code manual"*, deliverable D10 of the WAHALoads project, version October 2003.

Tiselj, I., Horvat, A., Černe, G., Gale, J., Parzer, I., Mavko, B., Giot, M., Seynhaeve, J.M., Kucienska, B., Lemonnier, H., *"WAHA3 code manual"*, deliverable D10 of the WAHALoads project, version March 2004.

Wylie, E.B., Streeter, V.L., *"Fluid Transients",* McGraw-Hill, 1978.

3.3. Work Package 3: Code validation and application

In the frame of ***WP 3***, eight organisations took part in a benchmark exercise, involving two types of codes:

- General purpose system codes, including a six equation two-fluid flow model with 1st order space and time integration, staggered mesh, and a library of fluid interface models based on flow regime maps;
- Specialised fast transient codes, including the two-phase homogeneous equilibrium model; they are of the 2nd order in space and time.

The benchmark exercise had several objectives:

- Evaluate the state-of-the-art of water-hammer-type transients simulations
- Identify deficiencies in existing codes.
- Define needs for further code developments.
- Provide reference cases for evaluating progress achieved in the course of the project.

For such purposes several test cases have been selected based on known theoretical benchmarks and existing experimental data. Additional benchmarks are under consideration. Each partner has expressed to which extent he could participate to some of these benchmarks, and with which code. The summary of the partners' commitments is indicated in the table hereunder.

Participant	*Codes*	*BM1.1a*	*BM1.1b*	*BM1.2a*	*BM1.2b*	*BM2*	*BM3*
CEA	CATHARE V1.5a rev.6	)	)	)	)	-	-
EA	RELAP5/mod3.2	-	)	-	-	)	-
EdF	EUROPLEXUS 2000	)	)	)	)	)	-
IJS	WAHA single phase	)	-	)	-	-	-
	TFTC (RELAP5 based)	-	)	-	)	)	-
TBL	RELAP5/mod3.3	)	)	)	)	)	)
UCL	DELOS	)	)	-	)	)	-
UMSICHT	MONA 2.2	)	)	)	)	)	)

The following table summarises the main key characteristics of the above mentioned codes.

CODE	Purpose of code		Order of numerical scheme		Time Integration Scheme			N° of equations	FSI
	General	Specific	*1st*	*2st*	Fully implicit	Partially implicit	Explicit		
CATHARE V1.5a rev.6	)	-	)	-	)	-	-	6	-
RELAP5	)	-	)	-	-	)	-	6	-
MONA 2.2	)	-	)	-	-	)	-	7	-
EUROPLEXUS 2000	-	)	-	)	-	-	)	3	)
WAHA single phase	-	)	-	)	-	-	)	3	-
TFTC (RELAP5 based)	-	)	-	)	-	-	)	6	-
DELOS	-	)	-	)	-	-	)	3	-

3.3.1. Description of the benchmark cases

- ***Theoretical test cases (BM1)***

The first case, labelled BM1.1, considers a highly simplified problem of a frictionless flow in a pipe instantaneously interrupted by a valve at the pipe outlet. The resulting transient consists in a compression wave travelling away from the valve back to the upstream reservoir and, after reflection on the constant pressure reservoir, in a decompression wave travelling back to the valve (**Fig.27**). For the cold liquid case (BM1.1a, T = 293 K) and in the absence of any damping effects, the cycle of compression and decompression wave continues without any attenuation of the amplitude of the pressure waves. For the hot liquid case (BM1.1b, T= 523 K), the response is more complicated and, as no analytical solution is available, the exercise consists in a cross-comparison of the code results.

The second theoretical case, labelled BM1.2, is also a highly simplified problem of a frictionless flow in a pipe instantaneously interrupted by a valve, but this time downstream of the valve. The resulting transient consists in a decompression wave travelling away from the valve towards the downstream reservoir and, after reflection on the constant pressure reservoir, in a compression wave travelling back to the valve.

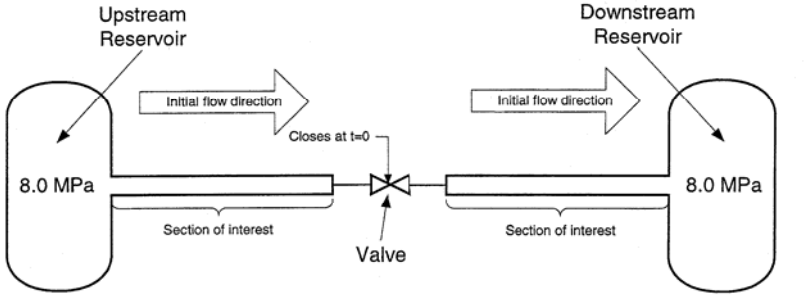

Fig.27.- Benchmark configurations (B.M. 1 and 2)

- ***Experimental test case (BM2)***

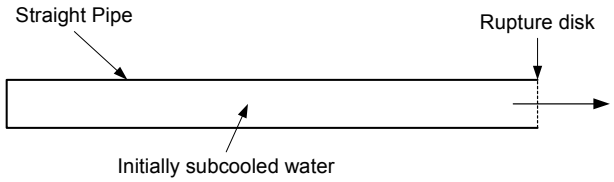

Fig.28.- Edwards' Pipe Blowdown (BM2)

This case is the well-known Edwards' pipe blowdown case (**Fig.28**) *(Straight Pipe Depressurisation Experiment)*, also known as the CSNI Standard Problem No.1. It consists of a pipe initially filled with pressurised sub-cooled water. The transient is initiated by bursting the rupture disk located at one end of the pipe. During the first phase of the transient, a rarefaction wave is travelling inside the pipe towards its closed end on which it is reflected. Later in the process, the blowdown is controlled by the strong evaporation of the liquid (flashing).

The objective of this test is to predict the propagation of the depressurisation wave, and in particular its reflection on the closed end with a noticeable pressure undershoot. It also

provides information on how flashing is predicted by the codes. Pressure, void fraction and trust force measurements are available for comparison.

- ***Experimental test case (BM3)***

The existing PPP test cases deal with the fast closure of valves in a steady-state liquid flow. A pump circulates water from a reservoir through a DN100 pipe approx. 200 m long. The transient is initiated by the rapid closure of a valve. During the first phase of the transient, a rarefaction wave is travelling inside the pipe towards the downstream reservoir. As a consequence, cavitation occurs downstream of the valve and a vapour bubble is formed just downstream of this valve. Upon reflection on the reservoir, the returning compression wave condenses the vapour bubble, inducing a cavitation hammer.

The objective of this test is to predict the propagation of the pressure waves and the resulting formation and collapse of the vapour bubble. It provides information on how flashing and condensation are predicted by the code. Pressure, force and void fraction measurements are available for comparison.

- ***Experimental data from WP1***

Existing codes and the WAHA code developed in WP2 have to be evaluated with the help of experimental data generated at three different facilities during the current project.

3.3.2. Results of the benchmark exercise

Deliverable 75 gives the detailed results of the benchmark exercise. The main conclusions are as follows:

For benchmark BM1A :

- 1st order codes with staggered grids: impact of numerical diffusion clearly visible in base case.
- Precision of 1st order codes can be improved by reducing the time step, little impact of number of nodes.
- 2nd order codes give sharper shock capturing with increased number of nodes.
- Most codes are capable of producing acceptable results, provided sufficient nodes and sufficiently small time steps are used. The MONA code is more diffusive.

For benchmark BM1B :

- General purpose system codes are more or less not capable of capturing secondary waves due to vapor cavity collapse.
- The origin of problem traced to physics package, not well adapted for rapid condensation, is suppressed to avoid stability problems.
- Special purpose codes for fast dynamic transients can capture condensation shock, but the amplitude is perhaps underestimated.

For benchmark BM2 :

- The rarefaction wave propagation is well predicted by all codes.
- Some problem with flashing model is observed in MONA code
- All codes predict higher pressure during the first phase of the transient.
- All codes predict some kind of a "void" wave traveling to closed end, whereas the experiment shows approximately constant pressure during first 0,2 s.
- The time when the pressure starts to drop depends on the model for critical flow at the break

For benchmark BM3 :

- Timing of the pressure pulses is well predicted.
- The amplitude of the first pressure pulses is slightly under predicted, except for BM3.1 pressure pulse after valve reopening.
- Some numerical problems: stability of the solution dependent on the initial void fraction and initial dissolved air fraction.

3.3.3. Conclusions

The benchmark exercises were found helpful for the first validation of the WAHA code, and the new detailed data obtained on three test facilities were used by the industrial partners for further verification of WAHA and of their own tools: DELOS, EUROPLEXUS, FLOWMASTER, MONA, RELAP5, ROLAST, and UMSICHT code. Fluid structure interaction effects have been studied using AGPIPE, ANSYS and EUROPLEXUS.
It is worth mentioning that the comparisons between the predictions and the data collected from the performed complex experiments have substantially increased the level of expertise of the scientists involved in this project and the qualification of the codes used mainly by the industrial partners.

4. Publication related to the WAHALoads project

BOGOI, A., SEYNHAEVE, J.M. and GIOT, M., "*Choked Flow Simulations by Means of a Two-Phase Two-Component Bubbly Flow Model with a Conservative Formulation"* 6th Workshop on Transport Phenomena in Two-Phase Flow, Bourgas, Sept. 11-16, 2001, 14 p.

GIOT, M., PRASSER, H.M., DUDLIK, A., EZSOL, G., HABIP, M., LEMONNIER, H., TISELJ, I., CASTRILLO, F., VAN HOVE, W., PEREZAGUA, R. & POTAPOV, S., "*Two-phase flow water hammer transients and induced loads on materials and structures of nuclear power plants (WAHALoads)"* FISA-2001 EU Research in Reactor Safety, Luxembourg 12-15 November 2001, EUR 20281, 176-187, G. VAN GOETHEM, A. ZURITA, J. MARTIN BERMEJO, P. MANOLATOS and H. BISCHOFF, Eds., EURATOM, 752p., 2002.

Altstadt, E., Carl, H., Weiss, R., *"Fluid-Structure Interaction Experiments at the Cold Water Hammer Test Facility (CWHTF) of Forschungszentrum Rossendorf"*, ANNUAL MEETING ON NUCLEAR TECHNOLOGY, 2002, 14 – 16 May, 2002, Stuttgart, Germany

KUCIENSKA, B., SEYNHAEVE, J.M., and GIOT M., *"Use of Extended Irreversible Thermodynamics to predict transient dissipative effects with the HEM and HRM models"*

40th European Two-Phase Flow Group Meeting in Stockholm and 2nd European Multiphase Systems Institute Meeting, 10-13 June 2002.

TISELJ, I. and HORVAT, A., *"Accuracy of the operator splitting technique for two-phase flow with stiff source terms"* 2002 ASME Fluids Engineering Division Summer Meeting, Montreal, Quebec, Canada, 14-18 July 2002.

GIOT, M., DUDLIK, A., LAUTER, E., LEMONNIER, H., TISELJ, I., CASTRILLO, F., VAN HOVE, W., PEREZAGUA, R., POTAPOV, S. and SEYNHAEVE, J.M., *"Two phase flow water hammer transients and induced loads on materials and structures (WAHALoads)"* CHISA 2002, 15th International Congress of Chemical and Process Engineering, 25-29 August 2002, Praha.

TISELJ, I., GALE, J., PARZER, I., "*Two-fluid model for analysis of water-hammer transient in elastic pipes"* presented at 2002 Winter Meeting of the American Nuclear Society, November 17-21, 2002, Washington. Trans. Am. Nucl. Soc., 2002, vol. 87, 239-241.

LEMONNIER, H., *"Two-fluid-1D-averaged model equations for a pipe undergoing arbitrary motions"*, Wahaload report CEA-T3.3-D61-301002, Technical report SMTH/LDTA/2002-043, CEA/Grenoble, France, submitted for publication to Multiphase Science and Technology, Begell.

DUDLIK, A., SCHONFELD, S.B.H., HAGEMANN, O., FAHLENKAMP, H., *"Water hammer and cavitational hammer in process plant pipe systems"*, CHISA 2002, 15th International Congress of Chemical and Process Engineering, 25 - 29 August 2002, Praha.

GALE, J., TISELJ, I., *"Water hammer in elastic pipes"* International Conference Nuclear Energy for New Europe 2002, Kranjska Gora Slovenia, September 9-12, 2002. Proceedings: Nuclear Society of Slovenia, Ljubljana, Paper 203, 8 p.

Prasser, H.-M., Böttger, A., Zschau, J., Baranyai, G., and Ezsöl, Gy., *"Thermal Effects During Condensation Induced Water Hammer Behind Fast Acting Valves In Pipelines"*, International Conference On Nuclear Engineering ICONE-11, 20-23 April, 2003, Shinjuku, Tokyo, Japan, paper no. ICONE11-36310

BOGOI, A., SEYNHAEVE, J.M., GIOT, M., *"A two-component two-phase bubbly flow model - Simulations of choked flows and water hammer"* 41th European Two-Phase Flow Group Meeting in Norway and 2nd European Multiphase Systems Institute Meeting, May 2003.

GIOT, M., SEYNHAEVE, J.M., *"The WAHALoads project : data, models and code"* 41th European Two-Phase Flow Group Meeting in Norway and 2nd European Multiphase Systems Institute Meeting, May 2003.

GIOT, M., SEYNHAEVE, J.M., *"Two-Phase Flow Water Hammer Transients : towards the WAHA code"* International Conference Nuclear Energy for New Europe 2003, Portoroz, Slovenia, September 8 – 11, 2003, Proceedings: Nuclear Society of Slovenia, Ljubljana, Paper 202, 8p.

GALE, A. and TISELJ, I., *"Modelling of 'cold' water hammer with WAHA Code"* International Conference Nuclear Energy for New Europe 2003, Portoroz, Slovenia, September 8 – 11, 2003, Proceedings: Nuclear Society of Slovenia, Ljubljana, Paper 214, 8p.

TISELJ, I., *"Numerical scheme of the WAHA code"* V: International Workshop on Advanced Numerical Methods for Multi-Dimensional Simulation of Two-Phase Flow: GRS Garching, Germany, 15-16 September 2003. [S.l.]: ASTAR, 2004, 10 p.

CITU-BOGOI, A., *"A Two-Phase, Two-Component Bubbly Flow Model"*, Université catholique de Louvain (UCL), Department of Mechanical Engineering, Doctoral thesis, September 2003.

GIOT, M., SEYNHAEVE, J.M., *"Simulation and experiments of two-phase flow water hammer transients"* 3rd European-Japanese Two-Phase Flow Group Meeting, Certosa di Pontignano, Italy, 21-27 September 2003, 6p.

TISELJ, I., GALE, J., HORVAT, A., PARZER, I., "*Characteristic and propagation velocities of the two-fluid models*" 10th International Topical Meeting on Nuclear Reactor Thermal Hydraulics, October 5-11, 2003, Seoul, Korea., Proceedings of NURETH-10.

GIOT, M., PRASSER, H.M., DUDLIK, A., EZSOL, G., JESCHKE, J., LEMONNIER, H., TISELJ, I., CASTRILLO, F., VAN HOVE, W., PEREZAGUA, R. & POTAPOV, S., *"Two-Phase Flow Water Hammer Transients and Induced Loads on Materials and Structures of Nuclear Power Plant (WAHALOADS)"* FISA-2003 EU Research in Reactor Safety, Luxembourg, November 2003.

Altstadt, E., H. Carl, R. Weiss, *"Fluid-Structure Interaction Investigations for Pipelines"*, Forschungszentrum Rossendorf, Report: FZR-393, December 2003

Dudlik, A., Schoenfeld, S.B.H., Hagemann, O., Carl, H., Prasser H.-M., *"Water Hammer and Condensation Hammer Scenarios in NPPs using new Measurement System",* 9th International Conference on Pressure Surges, 24 – 26 March, 2004, Chester, UK

KUCIENSKA, B., *"Friction Relaxation Model for Fast Transient Flow"* Université catholique de Louvain (UCL) Doctoral thesis, June 2004.

List of deliverables

No.[1]	Partner	Deliverable Title	Authors in case of report
D1	UCL	Minutes of the Start-up Meeting	M. Giot and J.M. Seynhaeve
D2	UCL	Half-yearly Report 1	M. Giot and J.M. Seynhaeve
D3	UCL	Half-yearly Report 2	M. Giot and J.M. Seynhaeve
D4	UCL	Mid-term Report	M. Giot and J.M. Seynhaeve
D5	UCL	Half-yearly Report 3	M. Giot and J.M. Seynhaeve
D6	UCL	Half-yearly Report 4	M. Giot and J.M. Seynhaeve
D7	UCL	final report	M. Giot and J.M. Seynhaeve
D8	UCL	Report on benchmark with homogeneous model	J.M. Seynhaeve

[1] Deliverable numbers: D1 – D81

D10	IJS CEA UCL	WAHA code manual	I. Tiselj, A. Horvart, J. Gale, I. Parzer, B. Mavco, M. Giot, J.M. Seynhaeve, B. Kucienska, H. Lemonnier
D11	FZR	Description of advanced two-phase flow instrumentation, wire-mesh sensors	H.M. Prasser, A. Böttger, J. Zschau
D12	FZR	Test report of advanced two-phase flow instrumentation, wire-mesh sensor	H.M. Prasser, A. Böttger, J. Zschau
D13	FZR	Documentation of advanced two-phase flow instrumentation adapted to PPP and PMK-2 facilities	H.M. Prasser, A. Böttger, J. Zschau
D14	FZR	Advanced two-phase flow instrumentation to PPP	Equipment delivered
D15	FZR	Advanced two-phase flow instrumentation to PMK-2	Equipment delivered
D16	FZR	Results of advanced two-phase flow instrumentation, PPP water hammer tests, cavitation caused by rapid valve closing	Described in chap 4.4
D17	FZR	Measurement data of advanced two-phase flow instrumentation at PPP water hammer tests, cavitation caused by rapid valve closing	Data available at UMSICHT
D18	FZR	Results of advanced two-phase flow instrumentation, PPP water hammer tests, condensation caused by cold water injection into steam (T1.8)	***See D37***
D19	FZR	Measurement data of advanced two-phase flow instrumentation, PPP water hammer tests, condensation caused by cold water injection into steam (T1.8)	See D37 and D38
D22	FZR	Description of CWHTF (T1.13)	E. Altstadt, R. Weiss
D23	FZR	ESR for stress measurements at CWHTF	E. Altstadt, R. Weiss
D24	FZR	QLR on stress measurements at CWHTF	E. Altstadt, H. Carl, R. Weiss
D25	FZR	DER on stress measurements at CWHTF	E. Altstadt, H. Carl, R. Weiss
D26	FZR	CWHTF data for code validation	E. Altstadt, H. Carl, R. Weiss
D27	FZR	Fluid structure interaction modelling in FE-code	E. Altstadt
D28	FZR	FE-code validation report	E. Altstadt
D29	FZR	Summary of achieved progress in 3D dynamic stress modelling under consideration of fluid structure interaction	E. Altstadt
D30	UMS	DER on existing water hammer data from PPP	T. Neuhaus, A. Dudlik
D31	UMS	Report on MONA benchmark calculations	T. Neuhaus, A. Dudlik
D32	UMS	Description of PPP test facility	A. Dudlik, R. Müller
D33	UMS	ESR on PPP water hammer tests, cavitation caused by rapid valve closing	A. Dudlik, R. Müller
D34	UMS	QLR on PPP water hammer tests, cavitation caused by rapid valve closing	A. Dudlik, R. Müller

D35	UMS	DER on PPP water hammer tests, cavitation caused by rapid valve closing	A. Dudlik
D36	UMS	Measurement data of PPP water hammer tests, cavitation caused by rapid valve closing (T1.7, T1.12)	A. Dudlik, R. Müller
D37	UMS	ESR on PPP water hammer tests, condensation caused by cold water injection into steam (T1.3, T1.8)	A. Dudlik, R. Müller
D38	UMS	QLR on PPP water hammer tests, condensation caused by cold water injection into steam (T1.8)	A. Dudlik
D40	UMS	Measurement data of PPP water hammer tests, condensation caused by cold water injection into steam (T1.8, T1.12)	Data available at UMSICHT
D41	UMS	ESR on PPP shock wave tests in two-phase flow caused by rapid valve action	A. Dudlik, R. Müller
D45	UMS	Model improvements and final validation of MONA	A. Dudlik, R. Müller
D46	AEKI	Description of PMK-2 test facility	L. Szabados, G. Baranyai, A. Guba, G. Ézsöl, L. Perneczky, I. Tóth, I. Trosztel
D47	AEKI	***ESR on PMK-2 water hammer tests, condensation caused by cold water injection into main steam-line of VVER-440-type PWR***	G. Ézsöl
D48	AEKI	***QLR on PMK-2 water hammer tests, condensation caused by cold water injection into main steam-line of VVER-440-type PWR***	H.M. Prasser, G. Ézsöl
D49	AEKI	***Results of advanced two-phase flow instrumentation, PMK-2 water hammer tests, condensation caused by cold water injection into main steam-line of VVER-440-type PWR***	See chap 4.5
D50	AEKI	***Measurement data of advanced two-phase flow instrumentation, PMK-2 water hammer tests, condensation caused by cold water injection into main steam-line of VVER-440-type PWR***	Data available at AEKI
D51	AEKI	DER on PMK-2 water hammer tests, condensation caused by cold water injection into main steam-line of VVER-440-type PWR	H.M. Prasser, G. Ézsöl
D52	AEKI	***Measurement data of PMK-2 water hammer tests, condensation caused by***	Data available at AEKI

		cold water injection into main steam-line of VVER-440-type PWR	
D55	FANP	UPTF data set for code validation	J. Jeschke
D56	FANP	Report on needs for new experiments on thermal-hydraulics and complex pipeline behaviour	E. Lauter, A Dudlik, G. Ezsol
D57	FANP	ROLAST-KWUROHR benchmark calculation results	E. Lauter
D58	FANP	ROLAST-KWUROHR model improvements and validation results	L. Gerstner, J. Jeschke
D59	FANP	Summary report on deficiencies of existing codes and models	J. Jeschke
D60	CEA	formulation of basic equation set for the WAHA code (T2.1)	In deliverable D10
D61	CEA	Report on benchmark with CATHARE	H. Lemonnier
D62	IJS	Numerical methods of WAHA code	I. Tiselj, G. Cerne, I. Parzer, A. Horvart
D63	IJS	WAHA code development interim report	I. Tiselj, G. Cerne, I. Parzer, A. Horvart
D64	IJS	Code development final	In deliverable D10
D65	IJS	WAHA code	Not a report
D66	IJS	WAHA pre- and postprocessors (T2.4)	Not a report
D67	IBER	Summary of achieved progress in thermal hydraulic modelling with respect to water hammer and shock waves	Not done by the partner
D68	IBER	Quality Assurance Manual	F. Castrillo
D69	FZR	Quality Assurance Audit	M. Prasser
D74	TBL	Technical Specification of Benchmark Test Cases	W. Van Hove
D75	TBL	Final Comparison Report of Benchmark Exercise	A. Cipollaro, W. Van Hove
D76	TBL	WAHA code validation results	A. Cipollaro, W. Van Hove
D77	EA	Report on benchmark calculations	
D78	EA	WAHA Code Validation results	*A. Rubbers, R. Perezagua*
D79	EA	Assessment on the results	A. Rubbers, R. Perezagua
D80	EdF	report on needs for new experiments on fluid-structure interaction and 3D dynamic stresses in walls of components	S. Potapov
D81	EdF	CIRCUS and PLEXUS validation report and comparison with WAHA Code (T3.4, T3.9, T3.12)	S. Potapov
D90	EdF	Report on the benchmark exercise (Plexus code)	S. Potapov
D91	IJS	Report on the benchmark exercise (Waha code)	I. Tiselj, G. Cerne